

Design, Synthesis, and Biological Evaluation of Novel 3-Aminomethylindole Derivatives as Potential Multifunctional Anti-Inflammatory and Neurotrophic Agents

Wei-Wei Wang,[†] Ting Liu,[†] Yu-Meng Lv, Wu-Yang Zhang, Zhi-Gang Liu, Jin-Ming Gao,^{*} and Ding Li^{*}



Cite This: *ACS Chem. Neurosci.* 2021, 12, 1593–1605



Read Online

ACCESS |



Metrics & More



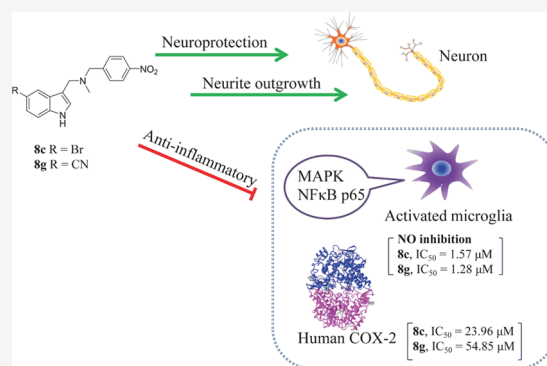
Article Recommendations



Supporting Information

ABSTRACT: The development of multifunctional molecules that are able to simultaneously interact with several pathological components has been considered as a solution to treat the complex pathologies of neurodegenerative diseases. Herein, a series of aminomethylindole derivatives were synthesized, and evaluation of their application for antineuroinflammation and promoting neurite outgrowth was disclosed. Our initial screening showed that most of the compounds potentially inhibited lipopolysaccharide (LPS)-stimulated production of NO in microglial cells and potentiated the action of NGF to promote neurite outgrowth of PC12 cells. Interestingly, with outstanding NO/TNF- α production inhibition and neurite outgrowth-promoting activities, compounds **8c** and **8g** were capable of rescuing cells after injury by H₂O₂. Their antineuroinflammatory effects were associated with the downregulation of the LPS-induced expression of the inflammatory mediators inducible nitric oxide synthase (iNOS) and cyclooxygenase-2 (COX-2). Western blotting and immunofluorescence assay results indicated that the mechanism of their antineuroinflammatory actions involved suppression of the MAPK/NF- κ B signal pathways. Further studies revealed that another important reason for the high comprehensive antineuroinflammatory activity was the anti-COX-2 capabilities of the compounds. All these results suggest that the potential biochemical multifunctional profiles of the aminomethylindole derivatives provide a new sight for the treatment of neurodegenerative diseases.

KEYWORDS: Neurodegenerative diseases, anti-inflammatory, neurite outgrowth, indole, COX-2, multifunction



1. INTRODUCTION

Neuroinflammation is indicated as one of the principal causes of the pathogenesis of several acute and chronic neurological disorders, such as Alzheimer's disease (AD) and Parkinson's disease (PD).^{1,2} The characteristics of neuroinflammation are attributed to the activation of microglia, astrocytes in the brain parenchyma, and the increase in inflammatory factors, such as chemokines, cytokines, and ROS/NOS, among others.^{3,4} Another significant characteristic is the interaction between glial cells and neurons; neurons upon an injury or a stimuli release factors that when perceived by glial cells can induce neuronal protection or neuroinflammation.^{4,5} However, the aberrant activation of microglia leads to extent of neuroinflammation and thereby triggers neuronal damage and the progression of neurodegenerative disease. Therefore, neuroinflammation in microglia might serve as an attractive therapeutic target to moderate the progression of inflammatory-mediated neurodegenerative diseases.^{6,7}

Neurotrophins, such as nerve growth factor (NGF), are a family of secreted proteins that play vital roles in promoting neural survival, regeneration, and differentiation throughout an individual's entire lifetime.^{8,9} Cumulative evidence suggests

that reduced neurotrophic support is a significant factor in the pathogenesis of neurodegenerative diseases.¹⁰ Therefore, neurotrophins are attractive candidates for therapeutic agents in chronic neurodegenerative diseases and acute injuries including trauma and strokes.¹¹ Unfortunately, therapeutic application of neurotrophins is severely restricted by their undesirable apoptotic effect through interactions with the p75^{NTR} receptor and poor penetration of the blood–brain barrier (BBB).¹² Thus, there is obviously a need for identification of small molecules that can mimic the neurotrophic action as an alternative therapy approach.^{9,13}

In recent years, multifunctional compounds that are able to simultaneously interact with several pathological components have been considered as a solution to treat the complex

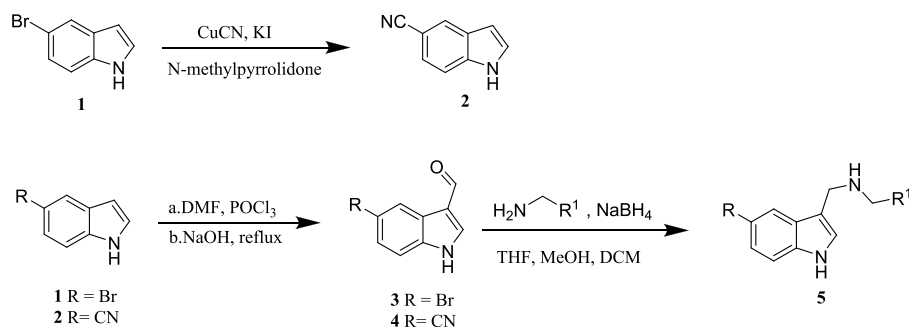
Received: February 9, 2021

Accepted: March 29, 2021

Published: April 22, 2021



Scheme 1. Synthesis of the 3-((Benzylamino)methyl)-1H-indole Derivatives 2 and 5



pathologies of neurodegenerative diseases.^{14,15} Discovery of antineuroinflammatory agents in combination with the induction of neurite outgrowth that promote neuronal survival, differentiation, and regeneration or potentiation of the actions of NGF might represent potential strategies for neurodegenerative disease treatment.^{16,17} Indole and its derivatives participate in a wide spectrum of biological activities, such as antimicrobial, anti-Alzheimer's disease, anti-inflammatory, antidepressant, antitumor, antioxidant, antiparkinsonian diseases, antimigraine activities.^{18,19} Indole derivatives have therefore captured the attention of organic synthetic chemists. Many anti-inflammatory agents containing indole scaffolds have been reported.^{18,19} For example, acemetacin and etodolac are nonsteroidal anti-cyclooxygenase (anti-COX) inhibitors that are used in the treatment of osteoarthritis and rheumatoid arthritis.¹⁹ However, few aminomethylindole derivatives have been reported for neuroinflammation or neurite outgrowth. Herein, we designed and synthesized three series of aminomethylindole derivatives. The structure–activity relationship studies on anti-inflammatory and neurotrophic effects were conducted, followed by the primary mechanisms of the active compounds. Taken together, all the data suggest that the multifunctional effects of the compounds provide a new insight for the treatment of neurodegenerative diseases.

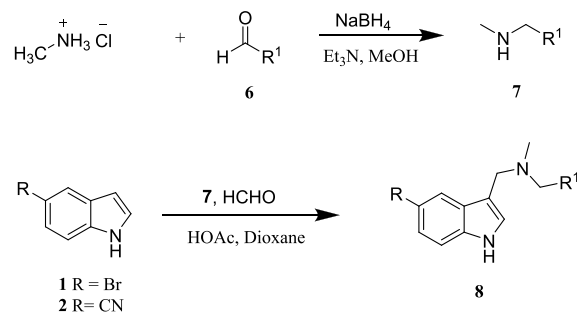
2. RESULTS AND DISCUSSION

2.1. Chemistry. The synthesis route for the 3-amino-methylindole derivative (5) is shown in Scheme 1. By use of the 5-bromoindole (1) as a raw material, compound 2 (5-cyano-1H-indole) was obtained by reaction with cuprous cyanide and a catalytic amount of KI in *N*-methylpyrrolidinone under N₂ (g).²⁰ The substituted indoles (1, 2) were submitted to a Vilsmeier–Haack reaction to furnish aldehydes (3, 4) in position 3 with 85–92% yields.²¹ Reductive amination of 1H-indole-3-carbaldehydes (3, 4) with the relevant substituted phenylmethanamine and sodium borohydride produced the target compound (5). The methanol/DCM/THF (1:2:1, v/v/v) solvent combination was used as a way to accelerate the reaction and achieved 60–90% yields.

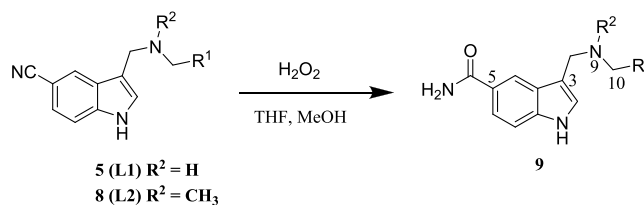
In parallel, the *N*-methyl-1-phenylmethanamine intermediate (7) was obtained from reductive amination of the relevant benzaldehyde (6) with the basified methylamine hydrochloride in a methanol solution. The substituted indoles 1 and 2 then underwent a Mannich reaction with the intermediate (7)²² and formaldehyde aqueous in 1,4-dioxane/glacial acetic acid solution to give the target compound (8) (Scheme 2).

Finally, as depicted in Scheme 3, hydrolysis of the relevant 5-cyano-1H-indole derivative 5 or 8 using hydrogen peroxide as an oxidant yielded the primary amide (9).

Scheme 2. Synthesis of the 3-((Benzylamino)methyl)-1H-indole Derivatives 7 and 8



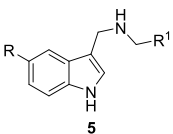
Scheme 3. Synthesis of the 1H-Indole-5-carboxamide Derivative 9



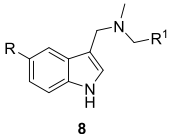
2.2. Inhibition of LPS-Induced NO Production in BV-2 Microglia Cells. Nitric oxide (NO), as a main signal molecule released in quantity by activated microglial, plays a vital role in neuroinflammation. Inhibition of NO overproduction is considered to be a significant indicator of antineuroinflammation.²³ Thus, a cytotoxicity assay was conducted using the MTT method, and the effect of the synthesized compounds on NO production in lipopolysaccharide (LPS)-induced BV-2 cells was evaluated using the Griess reagent. As shown in Table 1, cell viability did not change significantly after treatment with 10 μM concentrations of each compound, apart from 5g, 5h, and 5j. More importantly, lots of compounds were found to possess good inhibitory activities and IC₅₀ values of the test compounds, with an inhibition rate of more than 80% at 10 μM. Obviously, the inhibition effect of the compounds on NO production was divergent to a large extent, and it was dramatically influenced by different substituents on C5, N9, and C10. The primary structure–activity relationships on C5, N9, and the 4'-position of the phenyl ring for R¹ are described as follows:

(i) When the hydrogen on N9 was not methylated, the activity was determined by comprehensive factors of the substituents on C5 and the 4'-position of the phenyl ring. In general, unsubstituted phenyl and 4'-methoxyphenyl for R¹ did not produce a high inhibitory potency, whether the substituent

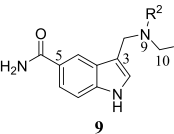
Table 1. Inhibitory Effects of Compounds 5a–5l, 8a–8l, 9a–k and the Control Curcumin on NO Production in LPS-Activated BV-2 Cells



5



8



9

Compd.	R/R ²	R ¹	NO	Cell viability	Compd.	R/R ²	R ¹	NO	Cell viability
			IC ₅₀ (μM) ^a	(%) ^b				IC ₅₀ (μM)	(%)
5a	R=Br		45.99 ± 4.48 % ^c	104.4 ± 2.1	8g	R=CN		1.28 ± 0.17	110.7 ± 7.7
5b	R=Br		48.10 ± 4.12 %	94.8 ± 0.8	8h	R=CN		51.18 ± 6.45 %	98.4 ± 1.2
5c	R=Br		1.41 ± 0.39	91.6 ± 1.3	8i	R=CN		3.04 ± 0.29	95.7 ± 1.8
5d	R=Br		1.97 ± 0.49	103.0 ± 4.2	8j	R=CN		2.53 ± 0.27	106.3 ± 0.6
5e	R=Br		3.37 ± 0.21	95.9 ± 8.6	8k	R=CN		40.72 ± 9.18 %	103.4 ± 3.7
5f	R=Br		77.95 ± 0.45%	101.3 ± 0.9	8l	R=CN		1.25 ± 0.42	101.5 ± 1.1
5g	R=CN		46.20 ± 0.73 %	88.6 ± 1.4	9a	R ² =H		24.47 ± 2.69 %	104.5 ± 3.9
5h	R=CN		63.29 ± 2.85 %	81.3 ± 2.1	9b	R ² =H		50.10 ± 12.98 %	93.2 ± 4.4
5i	R=CN		1.63 ± 0.15	95.0 ± 2.6	9c	R ² =H		63.08 ± 6.27 %	88.4 ± 1.2
5j	R=CN		51.27 ± 2.85 %	83.1 ± 2.1	9d	R ² =H		48.84 ± 0.45 %	95.5 ± 6.8
5k	R=CN		41.77 ± 1.32 %	93.9 ± 0.3	9e	R ² =H		6.67 ± 0.48	101.4 ± 2.1
5l	R=CN		3.22 ± 0.26	95.1 ± 5.0	9f	R ² =CH ₃		38.40 ± 2.69 %	97.8 ± 5.8
8a	R=Br		1.97 ± 0.08	94.1 ± 2.1	9g	R ² =CH ₃		45.99 ± 2.69 %	95.1 ± 2.1
8b	R=Br		1.49 ± 0.13	92.2 ± 0.9	9h	R ² =CH ₃		48.52 ± 3.58 %	96.8 ± 5.3
8c	R=Br		1.57 ± 0.66	108.5 ± 4.1	9i	R ² =CH ₃		63.08 ± 1.79 %	100.6 ± 6.8
8d	R=Br		1.35 ± 0.77	97.0 ± 2.4	9j	R ² =CH ₃		27.00 ± 2.90 %	97.5 ± 6.7
8e	R=Br		1.11 ± 0.13	91.3 ± 2.1	9k	R ² =CH ₃		52.95 ± 7.16 %	100.9 ± 8.5
8f	R=Br		1.80 ± 0.27	94.2 ± 3.2	curcumin			2.04 ± 0.17	99.2 ± 2.3

^aIC₅₀ value of each compound was defined as the concentration (μM) that caused 50% inhibition of NO production in LPS-activated BV-2 cells. ^bCell viability for LPS-activated BV-2 cells after treatment with 10 μM of each compound was assessed by MTT assay and was expressed as a percentage (%). ^cInhibition rate of each compound at 10 μM that inhibited NO production in LPS-activated BV-2 cells.

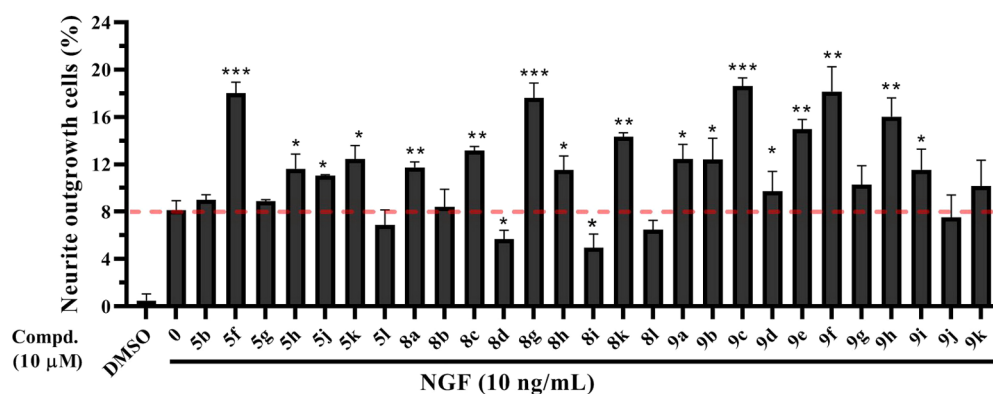


Figure 1. Effects of the prepared compounds on the NGF-induced neurite outgrowth in PC12 cells at 10 μ M. Data are the mean \pm standard error of three independent experiments: * p < 0.05, ** p < 0.01, and *** p < 0.001 compared with the NGF-induced group.

on C5 was a bromine, a cyano group, or a carbamoyl group. In the 5 series, with Br for C5 and Cl on the 4'-position of the phenyl ring, compound 5c (IC_{50} = $1.41 \pm 0.39 \mu$ M) had the best effect on the inhibition of NO production. Compared to 5c, a dramatic decrease in activity was seen by the introduction of a cyano group on C5 (compound 5h, inhibition rate = $63.29 \pm 2.85\%$ at 10 μ M). In contrast, when the substituent for R¹ was 4'-allyloxyphenyl and the Br group (compound 5f) was switched to a cyano group (compound 5l, IC_{50} = $3.22 \pm 0.26 \mu$ M), a significantly improved inhibitory activity was observed. In particular, compound 9e was the only one with relatively good activity in series 9, but it showed a lower activity than the parent compound 5l. This indicated that the hydrolysis of the relevant 5-cyano-1H-indole derivatives led to a significant reduction of the inhibitory potency. This occurrence was further verified from the screening results in Table 1.

(ii) Clearly, methylation of N9 in series 8 provided an impressive inhibitory potency. Many of these compounds showed high inhibitory activities with IC_{50} values of 1.11–1.97 μ M, such as 8a–8g, 8l. When the substituent on C5 was a bromine, it seemed that different groups at the 4'-position of the phenyl ring for R¹ did not weaken the powerful activity. In contrast, when the substituent on C5 was a cyano group, the inhibitory potency order was Cl > NO₂ > OCF₃ > OCH₂CHCH₂ > OCH₃ > H, followed by compounds 8l, 8g, 8j, 8i, 8h, and 8k. Similarly, it was revealed that hydrolysis of the cyano group quenched the inhibitory action.

Taking the data together, methylation of N9 was proved to be critical for the inhibition potency. On the other hand, the substituent on C5 was the second most important factor in the inhibition of NO production. Obviously, different combinations of substitutions on C5 and C10 showed significantly different inhibitory activities. Among them, compounds 5c, 5d, 5i, 8a–8g, and 8l yielded the corresponding IC_{50} values less than 2 μ M, which were superior to that of the positive control drug curcumin (IC_{50} = $2.04 \pm 0.17 \mu$ M).

2.3. Effect of Compounds on the Neurite Outgrowth of PC12 Cells. The rat pheochromocytoma cell line PC12 is widely used as a cell culture model for neuronal differentiation and survival.²⁴ The neuritogenic activities of the compounds were examined using PC12 cells. The cells were incubated with the compounds at a concentration of 10 μ M in combination with NGF (10 ng/mL). After 48 h of treatment, the cell viability was analyzed using an MTT assay, and the neurite-bearing cells were photographed under a light microscope and enumerated. The percentages of neurite-bearing cells induced

by the compounds, that did not exert detectable cytotoxicity, are shown in Figure 1. Notably, compounds 5f, 8c, 8g, 8k, 9c, 9e, 9f, and 9h greatly induced the formation and growth of neurites and profoundly increased the length of neurites in the presence of NGF (10 ng/mL). For instance, the percentage of neurite-bearing cells reached $13.2 \pm 0.3\%$ and $17.6 \pm 1.3\%$ for 8c and 8g, respectively. These values were significantly higher than those obtained from cells treated with 10 ng/mL NGF alone ($8.1 \pm 0.8\%$). The expression of the neuronal biomarker β -tubulin in 8c- and 8g-treated PC12 cells was also determined by the immunofluorescence assay experiments. As shown in Figure 2, 8c and 8g effectively enhanced the effect of NGF on β -tubulin induction and promoted neuronal survival and differentiation. These results indicated that these compounds could enhance the activity of NGF on neuritogenesis.

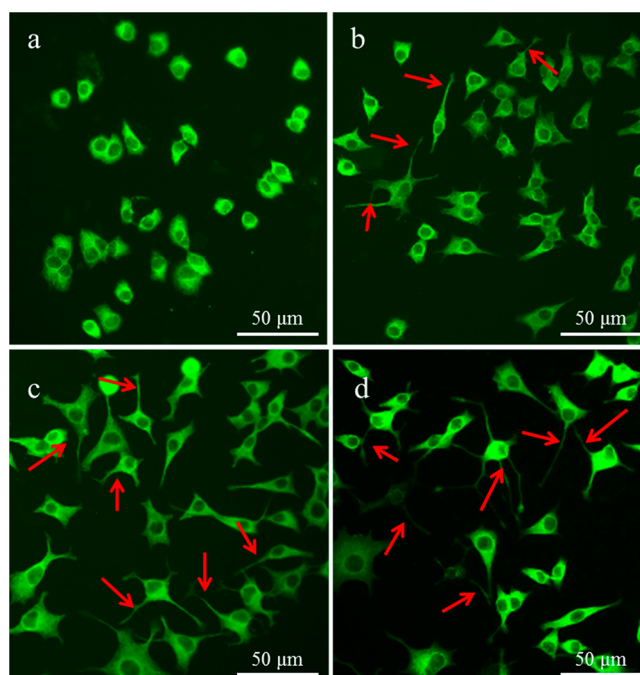


Figure 2. Immunofluorescence staining of neuronal biomarker β -tubulin. The morphological characteristics were observed under an OLYMPUS fluorescence microscope (20 \times): (a) control, (b) NGF (10 ng/mL), (c) 8c (10 μ M) + NGF (10 ng/mL), and (d) 8g (10 μ M) + NGF (10 ng/mL).

The pharmacological effect can be dramatically affected by multiple substituted groups and the type of the substituent. In contrast to the detrimental effect on the inhibition of LPS-induced NO production, the carbamoyl on the C5 of the indole ring potentially induced neurite outgrowth in PC12. For the case in which R² was H, compound **9c** with OCF₃ on the 4'-position of the phenyl ring for R¹ was the best for the neurite outgrowth of PC12 cells, followed by compound **9f** with CH₃ for R² and NO₂ on the 4'-position of the phenyl ring. Comparison of the bioactivity of compound **5f** showed that changing the bromine to a cyano group (**5l**) and the methylation of N9 (**8e** and **8i**) exhibited a significantly lower activity and even cytotoxicity. However, **8g** with methylation of N9 showed a higher activity than compound **5k**. On the basis of the above-mentioned analysis, it was suggested that the type of substituent on the C5 of the indole ring could endow the final structure with an excellent neurotogenic activity potential, but methylation of the N9 was not critical for the neurogenesis activity of the compounds.

In view of the comprehensive evaluation of the NO inhibition assay and neurite outgrowth assay, with outstanding biochemical activities, compounds **8c** and **8g** were selected for further tests to explore their effects on the protection against H₂O₂ and the production of inflammatory cytokine and to further dissect the underlying mechanisms.

2.4. Effects of Compounds on Protection against H₂O₂. Oxidative stress is a remarkable pathological indicator of neurodegenerative diseases. Cells of the nervous system are particularly vulnerable to oxidative stress-mediated damage.²⁵ H₂O₂ is used extensively as an inducer of oxidative stress *in vitro* because its cellular action and pathophysiological roles have been well studied.²⁶ The neuroprotective activities of compounds **8c** and **8g** against H₂O₂-induced oxidative stress were evaluated on PC12 cells at different concentrations. As shown in Figure 3, after incubation for 24 h, the cell viability of

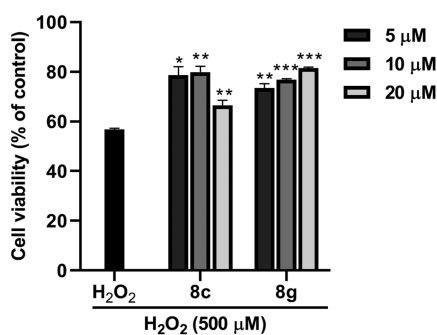


Figure 3. Neuroprotective effect of **8c** and **8g** on H₂O₂-induced PC12 cell death. Data are the mean \pm standard error of three independent experiments: **p* < 0.05, ***p* < 0.01, ****p* < 0.001 compared to the H₂O₂-treated group.

the PC12 cells exposed to 500 μM H₂O₂ was decreased to 56.9%. Both compounds **8c** and **8g** were capable of rescuing the cells after injury. The neuroprotective effect of **8c** was observed at concentrations of 5, 10, and 20 μM. The most potent concentration was 10 μM, and the cell viability was 79.9%. Compound **8g** could protect H₂O₂-induced cell damage in a dose-dependent manner.

2.5. Effects of Compounds on LPS-Induced TNF- α Production in BV-2 Cells and the Expression of iNOS and COX-2. A high concentration of NO is produced by the

stimulated inducible nitric oxide synthase (iNOS) and the levels of iNOS, cyclooxygenase-2 (COX-2), and tumor necrosis factor α (TNF- α), as principal proinflammatory mediators, also increased in the activated microglia.²³ Western blotting analysis and the enzyme-linked immunosorbent assay (ELISA) assay were employed to determine whether compounds **8c** and **8g** could further downregulate the expression of iNOS, COX-2, and TNF- α . As illustrated in Figure 4, the production of NO, iNOS, COX-2, and TNF- α markedly increased compared to that of the control group with LPS treatment (1 μg/mL). Compounds **8c** and **8g** not only specifically inhibited LPS-induced NO production but also suppressed the expressions of TNF- α , iNOS, and COX-2 in activated BV-2 cells in a concentration-dependent manner. Thus, the results indicated that compounds **8c** and **8g** were antineuroinflammatory agents.

2.6. Effects of Compounds on MAPK Signal Pathway. It has been reported that the mitogen-activated protein kinase (MAPK) pathway regulates the production of proinflammatory mediators.^{27,28} To confirm that the anti-inflammatory activities of **8c** and **8g** occurred through the regulation of the MAPK signaling transduction pathway, Western blotting experiments were conducted. As shown in Figure 5, the phosphorylation of ERK and JNK increased in the LPS-stimulated BV-2 cells. The significant reductions of the phosphorylated ERK and JNK were observed in both the 2 and 10 μM **8c** treatments. However, **8g** could significantly reduce the phosphorylation of ERK at a concentration of only 10 μM and slightly inhibited the phosphorylation of JNK. The phosphorylation of p38 was not affected by compounds **8c** and **8g** (data not shown). These results indicated that the MAPK signal pathway is involved in the antineuroinflammatory action of the 3-aminomethylindole derivatives.

2.7. Effects of Compounds on NF- κ B Signal Pathway. The transcription factor NF- κ B is a crucial transcriptional factor in the regulation of iNOS, COX-2, and TNF- α expression.^{27,28} To investigate the possible anti-inflammatory mechanisms of **8c** and **8g** further, the effects of the compounds on the NF- κ B pathway were examined. As shown in Figure 6, the levels of phosphorylated NF- κ B p65 were clearly increased by the LPS treatment. Compound **8c** significantly attenuated the phosphorylation of p65 in the LPS stimulated BV-2 cell nucleus at 10 μM, while **8g** significantly suppressed the phosphorylation of p65 in the nucleus at 2 and 10 μM. Evidently, **8g** was more efficient than **8c** in blocking the NF- κ B pathway. These findings were confirmed by immunofluorescence assay experiments (Figure 7). The results demonstrated that compounds **8c** and **8g** downregulated proinflammatory mediators by blocking the NF- κ B pathway.

2.8. COX-2 Inhibition Assay. Targeting cyclooxygenase 2 (COX-2) is an excellent strategy for developing nonsteroidal anti-inflammatory drugs (NSAIDs) to treat inflammation-related disorders.^{23,29} To test the COX-2 inhibitory effect of the synthesized compounds, COX-2 inhibitor screening assay was performed using commercial assay kits and celecoxib as a control. Fortuitously, the preliminary screening results suggested that 16 compounds with low IC₅₀ values for inhibition of the NO production exhibited different inhibitory activities on the COX-2 at 50 μM, as shown in Figure 8A. Some of the compounds were endowed with good identified inhibitory powers, as evidenced by the impressive inhibition rates of compounds **5c** (61.8%), **5l** (74.3%), **8b** (60.8%), **8c** (71.7%), and **8f** (81.2%). As representatives, the IC₅₀ values of

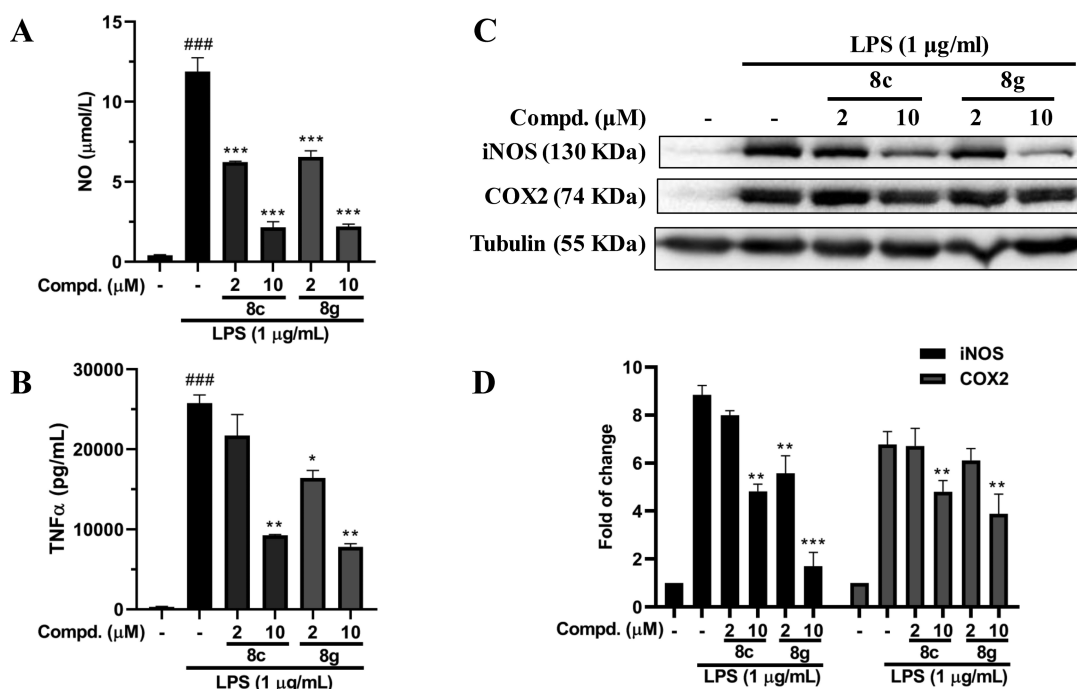


Figure 4. Anti-inflammatory effect of **8c** and **8g** in LPS-induced BV-2 cells. (A, B) Effects of **8c** and **8g** on the production of nitric oxide (NO) and tumor necrosis factor α (TNF- α) in LPS-induced BV-2 cells. (C) Effects of **8c** and **8g** on the expression of iNOS and COX-2. (D) Densitometric analyses of the iNOS and COX-2. Cells were treated with compounds for 24 h. Data are the mean \pm standard error of three independent experiments: ### p < 0.001 vs untreated controls; * p < 0.05, ** p < 0.01, and *** p < 0.001 compared to the LPS-treated group.

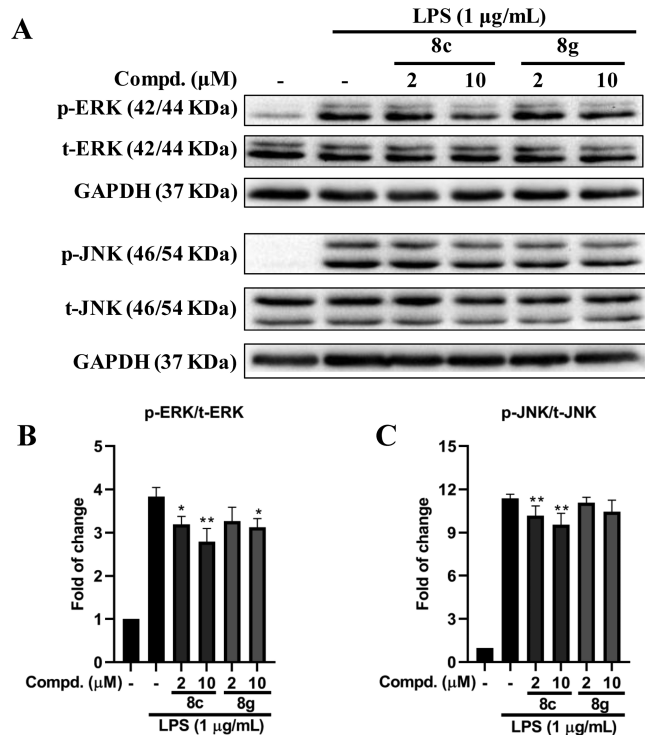


Figure 5. **8c** and **8g** attenuate the phosphorylation of ERK and JNK in LPS-induced BV-2 cells: (A) levels of ERK and JNK expressed as changes relative to the control group; (B, C) densitometric analyses of ERK and JNK. Cells were treated with compounds for 1 h. Data are the mean \pm standard error of three independent experiments: * p < 0.05, ** p < 0.01 compared to the LPS-treated group.

the compounds **8c** and **8g** were further determined (Figure 8B and Figure 8C). Compound **8c** showed moderate anti-COX-2

activity with an IC_{50} value of $23.96 \pm 4.99 \mu\text{M}$, which was better than that of **8g** ($IC_{50} = 54.85 \pm 7.38 \mu\text{M}$). Given that **8c** and **8g** could suppress the expression of COX-2 in activated BV-2 cells, moderate anti-COX-2 capabilities of the compounds may also be an important reason for their high comprehensive antineuroinflammatory activities.

3. CONCLUSION

In summary, three series of aminomethylindole derivatives were designed and synthesized. Several biological assays were conducted, which proved that the aminomethylindole derivatives can act as multifunctional agents to treat neuroinflammation and mimic the neurotrophic action. In the inhibition of NO production assay, most of the compounds exhibited diverse inhibitory effects with IC_{50} values ranging from 1.11 to greater than $10 \mu\text{M}$. Among these, 11 compounds showed significantly better inhibition of NO production than curcumin. In the neurite outgrowth assay, eight compounds greatly induced the formation and growth of neurites and profoundly increased the length of the neurites in the presence of NGF (10 ng/mL). The detailed structure–activity relationships suggested that the methylation of the N9 was critical for the NO production inhibition potency, and the type of substituent on the C5 of indole ring could endow the final structure with an excellent neurotogenic activity potential. On the basis of the comprehensive NO production inhibition and neurite outgrowth-promoting activities, compounds **8c** and **8g** were chosen for further studies. ELISA assay and Western blotting analyses further showed that **8c** and **8g** significantly suppressed the expression of TNF- α and downregulated the expressions iNOS and COX-2 in activated BV-2 cells in a concentration-dependent manner. In addition, the immunofluorescence assay reconfirmed that **8c** and **8g** could potentiate the actions of NGF. Additionally, both compounds **8c** and **8g**

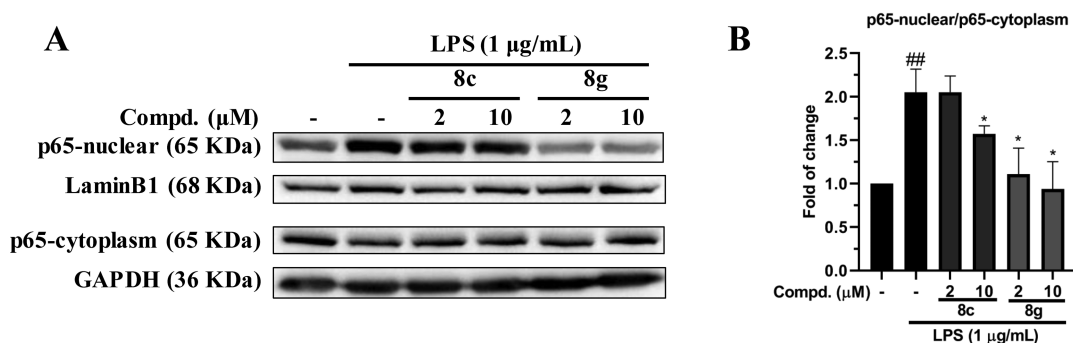


Figure 6. 8c and 8g downregulate proinflammatory mediators by blocking the NF- κ B pathway. (A) Levels of NF- κ B p65 in the nucleus and cytoplasm are expressed as a change relative to the control group. (B) Densitometric analyses of the NF- κ B p65 nuclear/cytoplasm. Cells were treated with compounds for 1 h. Data are the mean \pm standard error of three independent experiments: ^{###} $p < 0.01$ vs untreated controls; ^{*} $p < 0.05$, compared to the LPS-treated group.

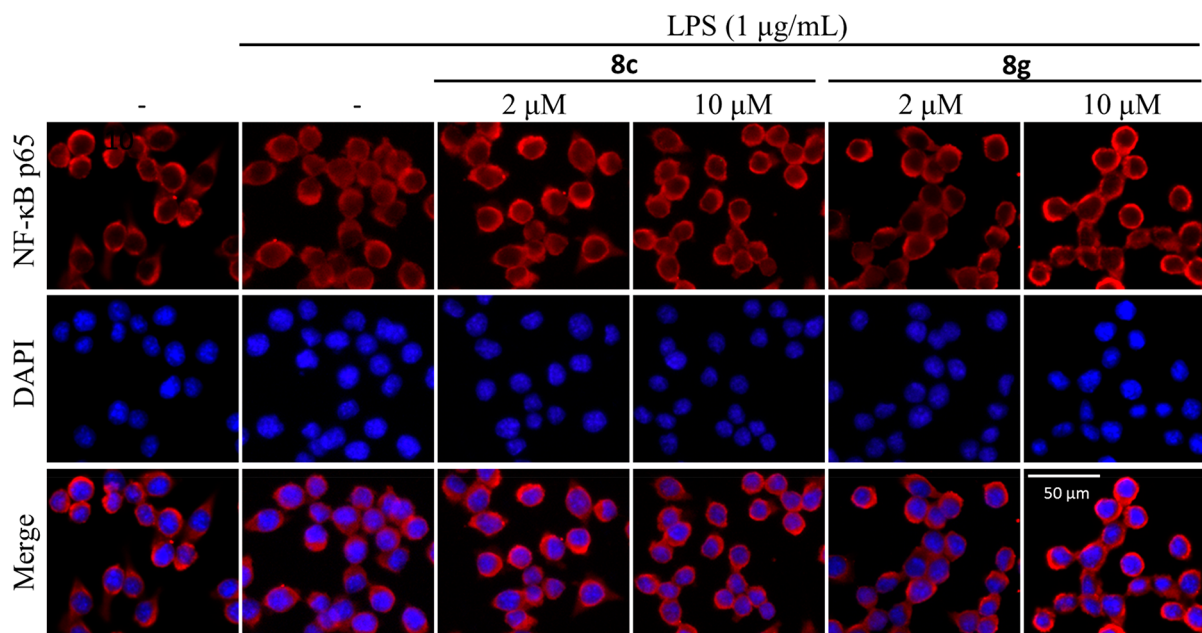


Figure 7. Immunofluorescence staining detected the distribution of NF- κ B p65 in both the nuclei and cytoplasm by some colocalization of receptors (p65, red) with the nuclei (DAPI, blue).

were capable of rescuing cells after injury by H₂O₂. Furthermore, the Western blotting and immunofluorescence assay indicated that the mechanism of their antineuroinflammatory action involved suppression of the MAPK/NF- κ B signal pathways. The COX-2 inhibition assay suggested that another important reason for the high comprehensive antineuroinflammatory activity was the anti-COX-2 capabilities of the compounds. In conclusion, the 3-aminomethylindole derivatives were proven to be effective antineuroinflammatory, neuroprotective, and neurotrophic agents. These findings opened up the new road for the treatment of neurodegenerative diseases.

4. METHODS

4.1. Chemistry. **4.1.1. General.** Carrying the lead drug candidates through the blood–brain barrier (BBB) is a major challenge, and it is a deciding factor for the development of novel neurotherapeutics.³⁰ The BBB permeability and druglikeness parameters of all designed compounds were predicted using admetSAR:³¹ a wide-ranging source for calculation of chemical ADMET properties of the compounds (Table S1, Supporting Information). Only the compounds with good

BBB permeability (BBB+) and druglikeness parameters were then synthesized.

All of the chemical reagents and solvents were purchased from commercial suppliers and used without further purification unless stated otherwise. The melting points were measured on an X-4 apparatus (Beijing Tech Instrument Co., Beijing, P. R. China) and were uncorrected. The ¹H and ¹³C NMR spectra were recorded on an Avance III 500 MHz instrument (Bruker, Karlsruhe, Germany). Chemical shifts (δ values) and coupling constants (J values) are given in parts per million and hertz, respectively. High resolution ESI-MS was performed on an AB SCIEX TripleTOF 5600+ LC/MS/MS system. All reactions were monitored by thin-layer chromatography (TLC), using precoated silica gel plates and ultraviolet light visualization. Crude products were purified by column chromatography using silica gel (200–300 mesh, Qingdao Marine Chemical Ltd., P. R. China).

4.1.2. Synthesis of 5-Cyano-1H-indole (2). A mixture of 5-bromoindole (1, 10.0 g, 0.051 mol), cuprous cyanide (7.9 g, 0.078 mol), and *N*-methylpyrrolidinone (vacuum distilled prior to use, 44 mL) was charged in a round-bottom flask under N₂ (g) and stirred at 155 °C for 6 h. After being naturally cooled to room temperature, the reaction system was quenched by the addition of cold water (20 mL) and filtered with diatomite. A solid precipitate was washed with 5%

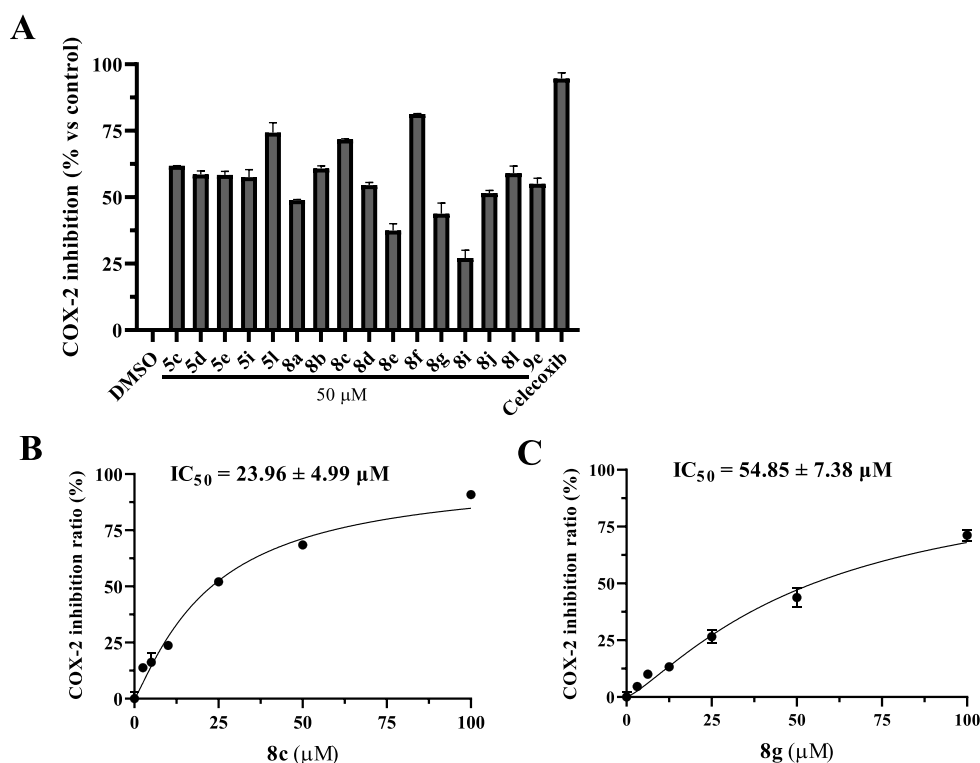


Figure 8. Effects of compounds on COX-2 activities. (A) Inhibition rate of the compounds at 50 μM . (B, C) IC_{50} values of **8c** and **8g** were calculated by the sigmoidal dose–response equation. Data are the mean \pm standard error of three independent experiments.

ammonium hydroxide until the aqueous layer was colorless, and then it was sequentially extracted with chloroform (20 mL) three times. The combined organic layers were washed with water and saturated aqueous sodium chloride and dried with MgSO_4 . The resulting crude would further be purified with column chromatography (silica gel, petroleum ether (PE):ethyl acetate (EA), 2:1 v/v) to give 5.8 g (80%) of 5-cyano-1*H*-indole (**2**) as a white solid (yield 99.59%). Mp: 106.1–108.0 $^{\circ}\text{C}$. ^1H NMR (500 MHz, CDCl_3): δ 8.59 (s, 1H), 8.01–7.98 (m, 1H), 7.48–7.41 (m, 2H), 7.36–7.33 (m, 1H), 6.65–6.63 (m, 1H). LRMS (ESI), m/z calcd for $\text{C}_9\text{H}_6\text{rN}_2$, $[\text{M} + \text{Na}]^+$ 307.10, found 307.88.

4.1.3. General Procedure for Synthesis of 1*H*-Indole-3-carbaldehyde Precursor (3, 4). Phosphorus oxychloride (POCl_3 , 1.2 mL, 12.75 mmol, 2.5 equiv) was added dropwise to previously cooled DMF (8.0 mL at 0–5 $^{\circ}\text{C}$) and stirred for 20 min. A solution of the relevant indole derivative (**1**, **2**, 5.1 mmol, 1 equiv) in DMF (20 mL) was added dropwise to the DMF– POCl_3 mixture. The mixture was then warmed to room temperature and stirred at 30 $^{\circ}\text{C}$ for 3 h. The reaction mixture was diluted with ice–water (50 mL), neutralized with 20% NaOH to a pH of 8–9, and stirred under reflux conditions overnight. The reactor was cooled down in an ice–water bath until solid precipitation appeared to have ceased. The precipitate in the mixture was then filtered off and purified by recrystallization from a 20% ethanol aqueous solution to give the compounds **3** and **4**.

Bromo-1*H*-indole-3-carbaldehyde (3). Crystalline powder; yield 90.81%. Mp: 204.1–205.2 $^{\circ}\text{C}$. ^1H NMR (500 MHz, MeOD): δ 9.88 (s, 1H), 8.30 (s, 1H), 8.11 (s, 1H), 7.41–7.36 (m, 2H). LRMS (ESI), m/z calcd for $\text{C}_9\text{H}_6\text{BrNO}$, $[\text{M} + \text{H}]^+$ 223.97; found 224.01.

3-Formyl-1*H*-indole-5-carbonitrile (4). Off-white crystalline powder; yield 92.19%. Mp: 248.3–249.8 $^{\circ}\text{C}$. ^1H NMR (500 MHz, MeOD): δ 9.97 (s, 1H), 8.54 (s, 1H), 8.28 (s, 1H), 7.66–7.55 (m, 2H). LRMS (ESI), m/z calcd for $\text{C}_{10}\text{H}_6\text{N}_2\text{O}$, $[\text{M} + \text{H}]^+$ 171.06, found 171.10.

4.1.4. General Procedure for Synthesis of 3-((Benzylamino)methyl)-1*H*-indole Derivative 5. First, relevant 1*H*-indole-3-carbaldehyde (**3–4**, 0.45 mmol, 1 equiv) was dissolved in 4 mL of 1:2:1 methanol/DCM/THF. Next, 4-substituted phenylmethanamine (0.54

mmol, 1.2 equiv) and freshly activated molecular sieves (4 \AA , 0.2 g) were added and the mixture was stirred under nitrogen at room temperature for 8–24 h. After imine formation, solvent was removed *in vacuo* and the crude material was dissolved in methanol. Approximately 34 mg of NaBH_4 (0.9 mmol, 2 equiv) was added under an ice bath, and the solution was stirred at 20 $^{\circ}\text{C}$ for 16 h.³² The completion of the reaction was monitored with the help of TLC. After the completion of the reaction, solvent was distilled off under a reduced pressure, and the residue was dissolved in 4 mL of ethyl acetate. The organic layer was then washed with saturated aqueous NaHCO_3 , dried over MgSO_4 , and concentrated *in vacuo*. The crude product was purified using flash chromatography with dichloromethane/methanol as eluents. The reaction mixture was worked up according to the general procedure and purified by column chromatography on silica gel to afford the compounds **5a–5l**.

***N*-Benzyl-1-(5-bromo-1*H*-indol-3-yl)methanamine (5a).** Yellow solid; yield 90.05%. Mp: 81.2–83.0 $^{\circ}\text{C}$. ^1H NMR (500 MHz, MeOD): δ 7.62 (d, $J = 1.5$ Hz, 1H), 7.27–7.11 (m, 8H), 3.78 (s, 2H), 3.68 (s, 2H). ^{13}C NMR (125 MHz, MeOD): δ 140.29, 136.50, 130.03, 129.52, 129.39, 128.12, 126.17, 125.16, 121.86, 113.90, 113.37, 113.09, 53.50, 43.75. LRMS (ESI), m/z calcd for $\text{C}_{16}\text{H}_{15}\text{BrN}_2$, $[\text{M} + \text{H}]^+$ 316.21, found 316.90.

1-(5-Bromo-1*H*-indol-3-yl)-*N*-(4-methoxybenzyl)methanamine (5b). White solid; yield 88.05%. Mp: 122.1–123.5 $^{\circ}\text{C}$. ^1H NMR (500 MHz, acetone): δ 10.25 (s, 1H), 7.85 (s, 1H), 7.35 (d, $J = 8.6$ Hz, 1H), 7.30 (d, $J = 8.5$ Hz, 3H), 7.20 (dd, $J = 8.6, 1.4$ Hz, 1H), 6.87 (d, $J = 8.5$ Hz, 2H), 3.92 (s, 2H), 3.77 (d, $J = 3.9$ Hz, 5H), 2.67 (s, 1H). ^{13}C NMR (125 MHz, acetone): δ 159.45, 136.37, 133.73, 129.99, 125.54, 125.38, 124.56, 122.45, 115.07, 114.24, 113.79, 112.22, 55.30, 52.99, 44.49. LRMS (ESI), m/z calcd for $\text{C}_{17}\text{H}_{17}\text{BrN}_2\text{O}$, $[\text{M} + \text{H}]^+$ 346.24, found 346.97.

1-(5-Bromo-1*H*-indol-3-yl)-*N*-(4-chlorobenzyl)methylamine (5c). White solid; yield 88.25%. Mp: 131.1–132.6 $^{\circ}\text{C}$. ^1H NMR (500 MHz, CDCl_3): δ 8.08 (s, 1H), 7.75 (s, 1H), 7.25 (d, $J = 13.5$ Hz, 5H), 7.19 (d, $J = 8.6$ Hz, 1H), 7.10 (s, 1H), 3.89 (s, 2H), 3.79 (s, 2H). ^{13}C NMR (126 MHz, CDCl_3): δ 138.97, 135.16, 132.79, 129.69, 129.03, 128.67, 125.21, 123.81, 121.90, 114.90, 113.03, 112.73, 52.79,

44.09. HRMS (ESI), m/z calcd for $C_{16}H_{14}BrClN_2$, $[M + H]^+$ 349.0102 (76.40%), 351.0080 (100.00%), found 349.0098 (76.08%), 351.0075 (100.00%).

1-(5-Bromo-1H-indol-3-yl)-N-(cyclohexylmethyl)methanamine (5d). Yellow solid; yield 70.25%. Mp: 57.0–58.5 °C. 1H NMR (500 MHz, $CDCl_3$): δ 8.79 (s, 1H), 7.79 (s, 1H), 7.28 (dd, $J = 8.8, 1.2$ Hz, 1H), 7.19 (d, $J = 8.6$ Hz, 1H), 7.09 (s, 1H), 3.94 (s, 2H), 2.59 (d, $J = 6.3$ Hz, 2H), 2.08 (d, $J = 6.2$ Hz, 1H), 1.77 (dd, $J = 24.6, 12.9$ Hz, 4H), 1.25 (ddd, $J = 31.8, 22.2, 14.2$ Hz, 5H), 0.96 (dd, $J = 24.1, 11.9$ Hz, 2H). ^{13}C NMR (125 MHz, $CDCl_3$): δ 135.10, 129.01, 124.91, 124.03, 121.52, 114.59, 112.81, 112.79, 56.58, 44.86, 37.89, 31.62, 26.76, 26.16. HRMS (ESI), m/z calcd for $C_{16}H_{21}BrN_2$, $[M + H]^+$ 321.0961 (100.00%), 323.0940 (98.94%); found 321.0955 (100.00%), 323.0934 (97.62%).

1-(5-Bromo-1H-indol-3-yl)-N-(4-(trifluoromethoxy)benzyl)methanamine (5e). White solid; yield 78.25%. Mp: 107.8–109.2 °C. 1H NMR (500 MHz, $CDCl_3$) δ 8.26 (s, 1H), 7.69 (d, $J = 1.4$ Hz, 1H), 7.28 (d, $J = 8.5$ Hz, 2H), 7.17 (dd, $J = 8.7, 1.8$ Hz, 1H), 7.08 (d, $J = 8.3$ Hz, 3H), 6.99 (s, 1H), 3.85 (s, 2H), 3.76 (s, 2H). ^{13}C NMR (125 MHz, $CDCl_3$): δ 148.33, 139.09, 135.15, 129.62, 128.98, 125.13, 123.93, 121.77, 121.66, 121.06, 119.62, 114.57, 112.95, 112.78, 52.70, 44.13. HRMS (ESI), m/z calcd for $C_{17}H_{14}BrF_3N_2O$, $[M + H]^+$ 399.0310 (100.00%), 401.0294 (99.34%), found 399.0302 (100.00%), 401.0285 (97.86%).

1-(5-Bromo-1H-indol-3-yl)-N-(4-(allyloxy)benzyl)methanamine (5f). Yellow oil; yield 65.20%. 1H NMR (500 MHz, $CDCl_3$): δ 8.24 (s, 1H), 7.71 (s, 1H), 7.31 (d, $J = 4.8$ Hz, 2H), 7.29 (d, $J = 1.4$ Hz, 1H), 7.24 (s, 1H), 7.19 (s, 1H), 6.96 (d, $J = 8.5$ Hz, 2H), 6.11 (m, 1H), 5.46 (d, $J = 17.2$ Hz, 1H), 5.33 (t, $J = 8.7$ Hz, 1H), 4.59 (d, $J = 5.3$ Hz, 2H), 3.80 (s, 2H), 3.76 (s, 2H). ^{13}C NMR (125 MHz, $CDCl_3$): δ 135.12, 133.56, 130.48, 129.65, 125.02, 124.79, 122.68, 117.76, 115.12, 114.69, 112.92, 112.55, 69.03, 68.11, 48.81. LRMS (ESI), m/z calcd for $C_{19}H_{19}BrN_2O$, $[M + H]^+$ 372.28, found 372.90.

3-((Benzylamino)methyl)-1H-indole-5-carbonitrile (5g). Yellow oil; yield 66.16%. 1H NMR (500 MHz, MeOD): δ 8.27 (s, 1H), 7.70 (d, $J = 8.6$ Hz, 1H), 7.54 (s, 1H), 7.47–7.21 (m, 6H), 4.39 (s, 2H), 4.17 (s, 2H). ^{13}C NMR (125 MHz, $CDCl_3$, MeOD): δ 138.66, 138.24, 128.89, 128.78, 127.87, 127.03, 126.59, 124.75, 124.45, 121.18, 113.09, 112.74, 101.84, 52.79, 42.93. LRMS (ESI), m/z calcd for $C_{17}H_{15}N_3$, $[M + H]^+$ 262.33; found 262.07.

3-(((4-Chlorobenzyl)amino)methyl)-1H-indole-5-carbonitrile (5h). Yellow oil; yield 66.62%. 1H NMR (500 MHz, $CDCl_3$): δ 8.88 (s, 1H), 8.03 (d, $J = 15.1$ Hz, 1H), 7.40–7.36 (m, 3H), 7.28 (d, $J = 3.7$ Hz, 3H), 7.23 (d, $J = 8.4$ Hz, 1H), 3.96 (s, 2H), 3.82 (s, 2H). ^{13}C NMR (125 MHz, $CDCl_3$): δ 138.62, 138.25, 132.87, 129.64, 128.68, 127.06, 125.27, 125.09, 124.86, 120.97, 115.79, 112.24, 102.48, 52.84, 43.98. LRMS (ESI), m/z calcd for $C_{17}H_{14}ClN_3$, $[M + H]^+$ 296.77, found 296.03.

3-(((4-(Trifluoromethoxy)benzyl)amino)methyl)-1H-indole-5-carbonitrile (5i). White solid; yield 78.16%. Mp: 99.4–101.1 °C. 1H NMR (500 MHz, $CDCl_3$) δ 8.36 (s, 1H), 8.00 (s, 1H), 7.37–7.33 (m, 2H), 7.33–7.28 (m, 2H), 7.18 (s, 1H), 7.10 (d, $J = 8.3$ Hz, 2H), 3.92 (s, 2H), 3.79 (s, 2H). ^{13}C NMR (100 MHz, $CDCl_3$): δ 148.35, 139.06, 138.18, 129.56, 127.13, 125.35, 125.29, 124.58, 121.13, 120.85, 116.23, 112.16, 102.92, 52.89, 44.23. HRMS (ESI), m/z calcd for $C_{18}H_{14}F_3N_3O$, $[M + H]^+$ 346.1161, found 346.1158.

3-(((4-Methoxybenzyl)amino)methyl)-1H-indole-5-carbonitrile (5j). Yellow oil; yield 85.35%. 1H NMR (500 MHz, $CDCl_3$): δ 7.94 (s, 1H), 7.34 (q, $J = 8.5$ Hz, 1H), 7.26–7.18 (m, 4H), 6.86 (dd, $J = 12.0, 8.6$ Hz, 3H), 3.79 (dd, $J = 9.3, 6.9$ Hz, 7H). ^{13}C NMR (125 MHz, $CDCl_3$): δ 159.03, 138.19, 134.25, 129.73, 129.30, 128.63, 125.34, 124.95, 124.90, 120.93, 114.12, 114.06, 112.26, 102.58, 55.38, 45.51, 43.34. LRMS (ESI), m/z calcd for $C_{18}H_{17}N_3O$, $[M + H]^+$ 292.35, found 292.09.

3-(((4-Nitrobenzyl)amino)methyl)-1H-indole-5-carbonitrile (5k). Yellow solid; yield 76.14%. Mp: 108.2–109.7 °C. 1H NMR (500 MHz, MeOD): δ 8.05 (d, $J = 0.8$ Hz, 2H), 7.46 (d, $J = 0.5$ Hz, 1H), 7.44 (s, 1H), 7.37–7.34 (m, 4H), 4.77 (s, 4H). ^{13}C NMR (125 MHz, MeOD): δ 140.12, 128.06, 127.10, 125.76, 125.34, 121.89, 117.68,

113.99, 113.51, 102.62, 56.75, 49.85. LRMS (ESI), m/z calcd for $C_{17}H_{14}N_4O_2$, $[2 M + Na]^+$ 635.66, found 635.02.

3-(((4-(Allyloxy)benzyl)amino)methyl)-1H-indole-5-carbonitrile (5l). Yellow solid; yield 56.23%. Mp: 40.0–41.0 °C. 1H NMR (500 MHz, $CDCl_3$): δ 9.50 (s, 1H), 7.99 (s, 1H), 7.37 (d, $J = 5.7$ Hz, 2H), 7.29 (d, $J = 8.5$ Hz, 2H), 7.26 (s, 1H), 6.92 (dd, $J = 13.2, 8.6$ Hz, 2H), 6.08 (m, 1H), 5.45 (d, $J = 17.3$ Hz, 1H), 5.32 (d, $J = 10.5$ Hz, 1H), 4.55 (t, $J = 6.6$ Hz, 2H), 4.01 (s, 2H), 3.86 (s, 2H). ^{13}C NMR (125 MHz, $CDCl_3$): δ 158.03, 138.16, 133.32, 131.24, 129.73, 126.98, 125.44, 124.91, 124.83, 120.96, 117.80, 114.87, 112.29, 102.36, 68.94, 52.54, 43.26. HRMS (ESI), m/z calcd for $C_{20}H_{19}N_3O$, $[M + H]^+$ 318.1601, found 318.1600.

4.1.5. General Procedure for Synthesis of the N-Methyl-1-phenylmethanamine Intermediate 7. A solution of methylamine hydrochloride (2.16 mmol, 1.2 equiv) in 2 mL of methanol was basified with 1.2 equiv of triethylamine for 30 min, and then the relevant aldehyde (1.8 mmol, 1 equiv) was added. The resulting solution was stirred at room temperature under the protection of inert gas for 24 h. After imine formation, the N-methyl-1-(4-substituted phenyl)methanamine intermediate 7 was prepared with yields of 92–95% according to the general procedure provided in section 4.1.4.

4.1.6. General Procedure for Synthesis of the 3-((Benzylaminomethyl)methyl)-1H-indole Derivative 8. A mixture of the indole derivative (1, 2, 0.562 mmol, 1 equiv), formaldehyde (65.5 μ L, 0.675 mmol, 1.2 equiv), 1,4-dioxane solution (2 mL), glacial acetic acid (0.8 mL), and the relevant N-methyl-1-phenylmethanamine intermediate 7 (1.2 equiv) was charged in a Schlenk tube under N_2 (g) and stirred at room temperature for 12 h. Once completion of reaction was obtained, as indicated by TLC, the reaction was quenched by saturated aqueous Na_2CO_3 and the product was extracted by dichloromethane. The organic layer was washed with distilled water and dried over $MgSO_4$, and solvent of the organic phase was evaporated under reduced pressure. The crude product was purified using flash chromatography with dichloromethane/methanol as eluents. The reaction mixture was worked up according to the general procedure and purified by column chromatography on silica gel to afford the compounds 8a–8l.

1-(5-Bromo-1H-indol-3-yl)-N-benzyl-N-methylmethylamine (8a). White solid; yield 63.06%. Mp: 122.3–124.2 °C. 1H NMR (500 MHz, $CDCl_3$): δ 8.07 (s, 1H), 7.84 (s, 1H), 7.38–7.31 (m, 4H), 7.28–7.24 (m, 2H), 7.22 (d, $J = 8.6$ Hz, 1H), 7.14 (s, 1H), 3.67 (s, 2H), 3.55 (s, 2H), 2.22 (s, 3H). ^{13}C NMR (125 MHz, MeOD): δ 139.79, 136.71, 130.95, 130.58, 129.30, 128.25, 127.14, 125.14, 122.63, 113.87, 113.09, 112.25, 62.59, 52.82, 42.41. HRMS (ESI), m/z calcd for $C_{17}H_{17}BrN_2$, $[M + H]^+$ 329.0648 (100.00%), 331.0627 (99.14%), found 329.0648 (100.00%), 331.0630 (95.43%).

1-(5-Bromo-1H-indol-3-yl)-N-(4-methoxybenzyl)-N-methylmethylamine (8b). Yellow solid; yield 72.18%. Mp: 98.5–100.2 °C. 1H NMR (500 MHz, $CDCl_3$) δ 8.37 (s, 1H), 7.78 (d, $J = 1.0$ Hz, 1H), 7.26 (d, $J = 8.5$ Hz, 2H), 7.22 (dd, $J = 8.7, 1.7$ Hz, 1H), 7.14 (d, $J = 8.6$ Hz, 1H), 7.05 (d, $J = 1.4$ Hz, 1H), 6.87 (d, $J = 8.5$ Hz, 2H), 3.79 (s, 3H), 3.63 (s, 2H), 3.49 (s, 2H), 2.19 (s, 3H). ^{13}C NMR (125 MHz, $CDCl_3$): δ 158.83, 135.09, 131.24, 130.44, 129.72, 124.90, 124.85, 122.38, 113.82, 113.27, 112.87, 112.62, 61.32, 55.40, 52.23, 42.25. HRMS (ESI), m/z calcd for $C_{18}H_{19}BrN_2O$, $[M + H]^+$ 359.0752 (100.00%), 361.0733 (99.57%), found 359.0743 (100.00%), 361.0725 (97.39%).

1-(5-Bromo-1H-indol-3-yl)-N-(4-nitrobenzyl)-N-methylmethylamine (8c). Yellow solid; yield 72.26%. Mp: 131.1–133.0 °C. 1H NMR (500 MHz, $CDCl_3$): δ 8.32 (s, 1H), 8.09 (dd, $J = 11.1, 5.6$ Hz, 2H), 7.67 (s, 1H), 7.40 (d, $J = 8.5$ Hz, 2H), 7.25–7.22 (m, 1H), 7.20 (d, $J = 8.6$ Hz, 1H), 7.01 (d, $J = 1.6$ Hz, 1H), 3.87 (s, 2H), 3.46 (s, 2H), 2.92 (s, 3H). ^{13}C NMR (125 MHz, DMSO): δ 147.90, 146.45, 135.07, 129.57, 129.27, 126.26, 123.44, 123.26, 121.28, 113.41, 111.11, 59.82, 52.19, 41.73. HRMS (ESI), m/z calcd for $C_{17}H_{16}BrN_3O_2$, $[M + H]^+$ 374.0495 (100.00%), 376.0478 (97.3%), found 374.0486 (100.00%), 376.0467 (97.27%).

1-(5-Bromo-1H-indol-3-yl)-N-(4-(trifluoromethoxy)benzyl)-N-methylmethylamine (8d). White solid; yield 65.04%. Mp: 96.6–97.7 °C. 1H NMR (500 MHz, MeOD): δ 8.29 (s, 1H), 7.70 (dd, $J = 8.6,$

1.4 Hz, 1H), 7.56 (s, 1H), 7.44 (d, $J = 8.6$ Hz, 1H), 7.36 (d, $J = 8.6$ Hz, 2H), 6.92 (d, $J = 8.6$ Hz, 2H), 4.39 (s, 2H), 4.14 (s, 2H), 3.75 (s, 3H). ^{13}C NMR (125 MHz, MeOD): δ 140.70, 133.28, 132.29, 130.53, 128.40, 127.26, 125.46, 123.59, 120.77, 116.27, 113.42, 108.19, 56.58, 51.98, 43.37. HRMS (ESI), m/z calcd for $\text{C}_{18}\text{H}_{16}\text{BrF}_3\text{N}_2\text{O}$, $[\text{M} + \text{H}]^+$ 413.0471 (100.00%), 415.0452 (99.56%), found 413.0473 (100.00%), 415.0459 (97.42%).

1-(5-Bromo-1H-indol-3-yl)-N-(4-(allyloxy)benzyl)-N-methylmethylamine (8e). White solid; yield 60.52%. Mp: 79.5–81.5 °C. ^1H NMR (500 MHz, CDCl_3): δ 8.26 (s, 1H), 7.79 (d, $J = 1.4$ Hz, 1H), 7.24 (dd, $J = 12.2, 5.1$ Hz, 3H), 7.17 (d, $J = 8.6$ Hz, 1H), 7.09 (d, $J = 1.9$ Hz, 1H), 6.89 (d, $J = 8.6$ Hz, 2H), 6.10–6.01 (m, 1H), 5.41 (dd, $J = 17.3, 1.4$ Hz, 1H), 5.29–5.25 (m, 1H), 4.53 (d, $J = 5.3$ Hz, 2H), 3.63 (s, 2H), 3.48 (s, 2H), 2.19 (s, 3H). ^{13}C NMR (125 MHz, CDCl_3): δ 157.88, 135.11, 133.56, 131.49, 130.40, 129.72, 124.96, 124.78, 122.44, 117.72, 114.67, 113.41, 112.92, 112.59, 69.02, 61.34, 52.31, 42.28. HRMS (ESI), m/z calcd for $\text{C}_{20}\text{H}_{21}\text{BrN}_2\text{O}$, $[\text{M} + \text{H}]^+$ 385.0910 (99.94%), 387.0890 (100.00%), found 385.0915 (98.81%), 387.0896 (100.00%).

1-(5-Bromo-1H-indol-3-yl)-N-(4-chlorobenzyl)-N-methylmethylamine (8f). White solid; yield 78.32%. Mp: 121.2–123.0 °C. ^1H NMR (500 MHz, CDCl_3): δ 8.20 (s, 1H), 7.88 (s, 1H), 7.33 (d, $J = 15.0$ Hz, 5H), 7.27 (d, $J = 8.6$ Hz, 1H), 7.18 (s, 1H), 3.72 (s, 2H), 3.55 (s, 2H), 2.25 (s, 3H). ^{13}C NMR (125 MHz, CDCl_3): δ 137.83, 135.12, 132.82, 130.50, 129.63, 128.54, 125.12, 124.76, 122.45, 113.10, 113.02, 112.63, 61.06, 52.68, 42.31. HRMS (ESI), m/z calcd for $\text{C}_{17}\text{H}_{16}\text{BrClN}_2$, $[\text{M} + \text{H}]^+$ 363.0258 (76.27%), 365.0238 (100.00%), found 363.0259 (77.13%), 365.0239 (100.00%).

3-((Methyl(4-nitrobenzyl)amino)methyl)-1H-indole-5-carbonitrile (8g). Yellow oil; yield 61.22%. ^1H NMR (500 MHz, CDCl_3): δ 8.64 (s, 1H), 8.17–8.12 (m, 3H), 7.49 (d, $J = 8.4$ Hz, 2H), 7.44 (s, 2H), 7.29 (s, 1H), 3.76 (s, 2H), 3.61 (s, 2H), 2.23 (s, 3H). ^{13}C NMR (100 MHz, CDCl_3): δ 147.41, 147.20, 138.26, 129.46, 127.54, 125.69, 125.53, 125.32, 123.68, 120.92, 114.65, 112.22, 102.88, 61.08, 53.25, 42.65. HRMS (ESI), m/z calcd for $\text{C}_{18}\text{H}_{16}\text{N}_4\text{O}_2$, $[\text{M} + \text{H}]^+$ 321.1346, found 321.1352.

3-(((4-Methoxybenzyl)amino)methyl)-1H-indole-5-carbonitrile (8h). White extract; yield 62.12%. ^1H NMR (500 MHz, MeOD): δ 9.19 (s, 1H), 7.86 (s, 1H), 7.24–7.18 (m, 2H), 7.11 (d, $J = 8.1$ Hz, 3H), 6.73 (d, $J = 8.5$ Hz, 2H), 3.64 (s, 4H), 3.56 (s, 2H), 3.38 (s, 2H), 2.06 (s, 3H). ^{13}C NMR (125 MHz, CDCl_3): δ 158.97, 138.27, 130.53, 130.30, 127.65, 126.21, 125.45, 124.82, 121.09, 113.86, 113.66, 112.24, 102.24, 61.19, 55.36, 51.94, 41.96. LRMS (ESI), m/z calcd for $\text{C}_{19}\text{H}_{19}\text{N}_3\text{O}$, $[\text{M} + \text{K}]^+$ 649.56, found 649.70.

3-(((4-(Allyloxy)benzyl)amino)methyl)-1H-indole-5-carbonitrile (8i). White extract; yield 61.42%. ^1H NMR (500 MHz, CDCl_3): δ 8.48 (s, 1H), 8.07 (s, 1H), 7.40 (q, $J = 8.5$ Hz, 2H), 7.25 (d, $J = 8.7$ Hz, 3H), 6.90 (d, $J = 8.5$ Hz, 2H), 6.06 (m, 1H), 5.42 (dd, $J = 17.2, 1.3$ Hz, 1H), 5.28 (d, $J = 10.8$ Hz, 1H), 4.54 (d, $J = 5.3$ Hz, 1H), 4.12 (d, $J = 7.1$ Hz, 1H), 3.68 (s, 2H), 3.50 (s, 2H), 2.20 (s, 3H). ^{13}C NMR (125 MHz, CDCl_3): δ 158.03, 138.16, 133.32, 131.24, 129.73, 126.98, 125.44, 124.91, 124.83, 120.96, 117.80, 114.87, 112.29, 102.36, 68.94, 65.01, 52.54, 43.26. HRMS (ESI), m/z calcd for $\text{C}_{21}\text{H}_{21}\text{N}_3\text{O}$, $[\text{M} + \text{H}]^+$ 332.1757, found 332.1752.

3-((Methyl(4-(trifluoromethoxy)benzyl)amino)methyl)-1H-indole-5-carbonitrile (8j). White oil; yield 62.05%. ^1H NMR (500 MHz, CDCl_3): δ 8.56 (s, 1H), 8.13 (s, 1H), 7.42 (s, 2H), 7.35 (d, $J = 8.5$ Hz, 2H), 7.25 (d, $J = 2.0$ Hz, 1H), 7.16 (d, $J = 8.1$ Hz, 2H), 3.71 (s, 2H), 3.52 (s, 2H), 2.20 (s, 3H). ^{13}C NMR (125 MHz, CDCl_3): δ 148.32, 138.28, 138.17, 130.22, 127.62, 125.80, 125.47, 125.18, 121.04, 120.93, 114.88, 112.14, 102.63, 61.14, 52.91, 42.45. HRMS (ESI), m/z calcd for $\text{C}_{19}\text{H}_{16}\text{F}_3\text{N}_3\text{O}$, $[\text{M} + \text{H}]^+$ 360.1318, found 360.1317.

3-((Benzyl(methyl)amino)methyl)-1H-indole-5-carbonitrile (8k). White solid; yield 76.85%. Mp: 134.1–136.0 °C. ^1H NMR (500 MHz, CDCl_3): δ 8.57 (s, 1H), 8.06 (s, 1H), 7.38 (dd, $J = 8.1, 4.7$ Hz, 2H), 7.35–7.32 (m, 4H), 7.25 (m, 2H), 3.68 (s, 2H), 3.54 (s, 2H), 2.21 (s, 3H). ^{13}C NMR (125 MHz, CDCl_3): δ 139.21, 138.22, 129.18, 128.45, 127.68, 127.25, 125.86, 125.46, 125.10, 121.06, 114.97,

112.05, 102.58, 62.11, 52.49, 42.51. LRMS (ESI), m/z calcd for $\text{C}_{18}\text{H}_{17}\text{N}_3$, $[\text{M} + \text{H}]^+$ 276.36, found 276.11.

3-(((4-Chlorobenzyl)amino)methyl)-1H-indole-5-carbonitrile (8l). White solid; yield 70.62%. Mp: 105.5–107.2 °C. ^1H NMR (500 MHz, CDCl_3): δ 8.51 (s, 1H), 8.09 (s, 1H), 7.42–7.37 (m, 2H), 7.29–7.22 (m, 5H), 3.68 (s, 2H), 3.48 (s, 2H), 2.17 (s, 3H). ^{13}C NMR (125 MHz, CDCl_3): δ 138.27, 137.81, 132.85, 130.36, 128.56, 127.65, 125.81, 125.47, 125.19, 121.01, 114.88, 112.12, 102.69, 61.26, 52.75, 42.41. HRMS (ESI), m/z calcd for $\text{C}_{18}\text{H}_{16}\text{ClN}_3$, $[\text{M} + \text{H}]^+$ 310.1105, found 310.1106.

4.1.7. General Procedure for Synthesis of the 1H-Indole-5-carboxamide Derivative 9. Hydrogen peroxide and 20% NaOH were added dropwise to a solution of the relevant 5-cyano-1H-indole derivative 8 or 9 (30 mg), respectively, in 200 μL of methanol/THF (3:17, v/v) at -5 °C.³³ The mixture was warmed to room temperature and stirred at 25 °C for 24 h. After completion of the reaction, it was then diluted with distilled water and extracted with dichloromethane. The dichloromethane extracts were washed with saturated brine, dried over anhydrous MgSO_4 , concentrated *in vacuo*, and purified by column chromatography on silica gel to afford the target compounds 9a–9k.

3-((Benzylamino)methyl)-1H-indole-5-carboxamide (9a). Yellow solid; yield 52.86%. Mp: 199.1–201.0 °C. ^1H NMR (500 MHz, MeOD): δ 8.27 (s, 1H), 7.70 (d, $J = 8.6$ Hz, 1H), 7.54 (s, 1H), 7.47–7.35 (m, 6H), 4.39 (s, 2H), 4.17 (s, 2H). ^{13}C NMR (125 MHz, MeOD): δ 173.60, 140.00, 133.71, 130.82, 130.30, 130.19, 129.49, 127.72, 126.50, 122.75, 120.01, 112.63, 108.11, 54.78, 43.03. LRMS (ESI), m/z calcd for $\text{C}_{17}\text{H}_{17}\text{N}_3\text{O}$, $[\text{M} + \text{H}]^+$ 280.34, found 280.05.

3-(((4-Chlorobenzyl)amino)methyl)-1H-indole-5-carboxamide (9b). Yellow oil; yield 51.56%. ^1H NMR (500 MHz, MeOD): δ 8.30 (s, 1H), 7.71 (d, $J = 8.6$ Hz, 1H), 7.56 (s, 1H), 7.47–7.42 (m, 3H), 7.40 (d, $J = 8.4$ Hz, 2H), 4.42 (s, 2H), 4.19 (s, 2H). ^{13}C NMR (125 MHz, MeOD): δ 173.57, 139.98, 136.37, 132.62, 132.17, 130.26, 129.72, 127.68, 126.52, 124.29, 122.79, 120.03, 112.65, 54.78, 43.11. LRMS (ESI), m/z calcd for $\text{C}_{17}\text{H}_{16}\text{ClN}_3\text{O}$, $[\text{M} + \text{H}]^+$ 314.79; found 314.01.

3-(((4-(Trifluoromethoxy)benzyl)amino)methyl)-1H-indole-5-carboxamide (9c). White solid; yield 51.40%. Mp: 88.5–90.0 °C. ^1H NMR (500 MHz, MeOD): δ 8.28 (s, 1H), 7.71 (dd, $J = 8.6, 1.3$ Hz, 1H), 7.49 (d, $J = 8.5$ Hz, 2H), 7.46–7.41 (m, 2H), 7.27 (d, $J = 8.1$ Hz, 2H), 4.17 (s, 2H), 3.99 (s, 2H). ^{13}C NMR (125 MHz, MeOD): δ 173.85, 150.13, 140.13, 137.35, 131.88, 127.90, 127.64, 125.83, 122.92, 122.44, 122.20, 120.13, 112.43, 112.34, 52.15, 43.85. LRMS (ESI), m/z calcd for $\text{C}_{18}\text{H}_{16}\text{F}_3\text{N}_3\text{O}_2$, $[\text{M} + \text{H}]^+$ 364.34, found 364.02.

3-(((4-(Methoxybenzyl)amino)methyl)-1H-indole-5-carboxamide (9d). Yellow oil; yield 53.34%. ^1H NMR (500 MHz, MeOD): δ 8.27 (s, 1H), 7.71 (d, $J = 8.6$ Hz, 1H), 7.56 (s, 1H), 7.46 (d, $J = 8.6$ Hz, 1H), 7.35 (dd, $J = 15.8, 8.5$ Hz, 2H), 6.94 (dd, $J = 8.5, 3.3$ Hz, 2H), 4.41 (s, 2H), 4.15 (s, 2H), 3.77 (s, 3H). ^{13}C NMR (125 MHz, MeOD): δ 173.56, 162.05, 139.97, 132.50, 131.51, 129.75, 127.66, 126.59, 124.64, 124.21, 122.79, 119.99, 115.56, 112.67, 107.39, 55.83, 54.78, 42.60. LRMS (ESI), m/z calcd for $\text{C}_{18}\text{H}_{19}\text{N}_3\text{O}_2$, $[\text{M} + \text{H}]^+$ 310.37, found 310.03.

3-(((4-(Allyloxy)benzyl)amino)methyl)-1H-indole-5-carboxamide (9e). White oil; yield 50.02%. ^1H NMR (500 MHz, MeOD): δ 8.05 (s, 1H), 7.54 (t, $J = 4.1$ Hz, 2H), 7.43 (d, $J = 8.5$ Hz, 1H), 7.33 (d, $J = 8.5$ Hz, 2H), 6.96 (d, $J = 8.5$ Hz, 2H), 6.05 (m, 1H), 5.39 (dd, $J = 17.3, 1.3$ Hz, 1H), 5.25 (dd, $J = 10.6, 1.0$ Hz, 1H), 4.56 (d, $J = 5.0$ Hz, 2H), 4.19 (s, 2H), 3.96 (s, 2H). ^{13}C NMR (125 MHz, MeOD): δ 171.32, 160.20, 139.81, 134.78, 131.73, 129.86, 129.19, 128.11, 125.65, 125.39, 121.67, 117.56, 116.05, 113.80, 111.22, 69.80, 52.15, 42.87. HRMS (ESI), m/z calcd for $\text{C}_{20}\text{H}_{21}\text{N}_3\text{O}_2$, $[\text{M} + \text{H}]^+$ 336.1706, found 336.1710.

3-((Methyl(4-nitrobenzyl)amino)methyl)-1H-indole-5-carboxamide (9f). Yellow oil; yield 50.62%. ^1H NMR (500 MHz, DMSO): δ 11.17 (s, 1H), 8.28 (s, 1H), 8.17 (d, $J = 8.6$ Hz, 2H), 7.82 (s, 1H), 7.64 (dd, $J = 18.0, 8.5$ Hz, 3H), 7.35 (d, $J = 8.5$ Hz, 2H), 7.09 (s, 1H), 3.75 (s, 2H), 3.64 (s, 2H), 2.14 (s, 3H). ^{13}C NMR (125 MHz, DMSO): δ 169.09, 146.44, 138.72, 137.94, 129.54, 126.97, 125.87, 124.92, 123.27, 120.78, 119.52, 112.38, 110.68, 59.83, 59.73, 52.33,

41.77. LRMS (ESI), m/z calcd for $C_{18}H_{18}N_4O_3$, $[M + H]^+$ 339.37, found 339.10.

3-((4-Methoxybenzyl)(methylamino)methyl)-1H-indole-5-carboxamide (**9g**). Yellow solid; yield 55.32%. Mp: 69.8–71.5 °C. 1H NMR (500 MHz, MeOD): δ 8.23 (s, 1H), 7.68 (dd, $J = 8.6, 1.3$ Hz, 1H), 7.42 (d, $J = 8.6$ Hz, 1H), 7.35–7.29 (m, 1H), 7.25 (d, $J = 8.5$ Hz, 2H), 6.89 (d, $J = 8.5$ Hz, 2H), 3.83 (s, 2H), 3.78 (s, 3H), 3.58 (s, 2H), 2.24 (s, 3H). ^{13}C NMR (125 MHz, MeOD): δ 174.01, 160.64, 140.11, 132.02, 130.66, 128.79, 127.75, 125.57, 122.18, 120.69, 114.79, 112.92, 112.16, 61.72, 55.68, 52.62, 41.91. LRMS (ESI), m/z calcd for $C_{19}H_{21}N_3O_2$, $[M + H]^+$ 324.40, found 324.07.

3-(((4-Allyloxy)benzyl)(methylamino)methyl)-1H-indole-5-carboxamide (**9h**). Yellow solid; yield 50.14%. Mp: 89.1–91.0 °C. 1H NMR (500 MHz, MeOD): δ 8.23 (s, 1H), 7.71 (d, $J = 8.7$ Hz, 1H), 7.60 (s, 1H), 7.47 (d, $J = 8.6$ Hz, 1H), 7.37 (d, $J = 8.5$ Hz, 2H), 6.98 (d, $J = 8.4$ Hz, 2H), 6.02 (m, 1H), 5.36 (dd, $J = 17.3, 1.4$ Hz, 1H), 5.22 (dd, $J = 10.6, 1.2$ Hz, 1H), 4.54 (d, $J = 5.1$ Hz, 2H), 4.45 (s, 2H), 4.20 (s, 2H), 2.63 (s, 3H). ^{13}C NMR (125 MHz, MeOD): δ 173.48, 161.18, 140.02, 134.57, 133.43, 130.87, 128.32, 126.90, 122.87, 120.04, 117.74, 116.39, 112.80, 69.87, 60.16, 51.88, 39.50. LRMS (ESI), m/z calcd for $C_{21}H_{23}N_3O_2$, $[M + H]^+$ 350.43, found 350.06.

3-((Methyl(4-(trifluoromethoxy)benzyl)amino)methyl)-1H-indole-5-carboxamide (**9i**). Yellow solid; yield 56.07%. Mp: 61.5–63.0 °C. 1H NMR (500 MHz, MeOD): δ 8.31 (d, $J = 1.0$ Hz, 1H), 7.69 (dd, $J = 8.6, 1.6$ Hz, 1H), 7.46 (d, $J = 8.6$ Hz, 2H), 7.43 (d, $J = 8.6$ Hz, 1H), 7.38 (s, 1H), 7.24 (d, $J = 8.1$ Hz, 2H), 3.94 (s, 2H), 3.72 (s, 2H), 2.30 (s, 3H). ^{13}C NMR (125 MHz, MeOD): δ 173.96, 149.93, 140.18, 132.39, 128.71, 128.03, 125.69, 122.25, 121.97, 120.78, 112.23, 61.16, 53.21, 41.80. LRMS (ESI), m/z calcd for $C_{19}H_{18}F_3N_3O_2$, $[M + H]^+$ 378.37, found 378.07.

3-((Benzyl(methylamino)methyl)-1H-indole-5-carboxamide (**9j**). White solid; yield 58.08%. Mp: 96.0–98.0 °C. 1H NMR (500 MHz, MeOD): δ 8.27 (s, 1H), 7.71 (dd, $J = 8.6, 1.4$ Hz, 1H), 7.46–7.42 (m, 2H), 7.36 (dt, $J = 15.6, 7.4$ Hz, 5H), 4.04 (s, 2H), 3.83 (s, 2H), 2.38 (s, 3H). ^{13}C NMR (125 MHz, MeOD): δ 173.83, 140.08, 131.13, 129.67, 129.19, 128.71, 128.64, 125.94, 122.39, 120.51, 112.36, 110.95, 61.80, 52.67, 41.34. LRMS (ESI), m/z calcd for $C_{18}H_{19}N_3O$, $[M + H]^+$ 294.37, found 294.02.

3-(((4-Chlorobenzyl)(methylamino)methyl)-1H-indole-5-carboxamide (**9k**). White solid; yield 59.35%. Mp: 160.3–162.0 °C. 1H NMR (500 MHz, MeOD): δ 8.29 (s, 1H), 7.71 (dd, $J = 8.6, 1.4$ Hz, 1H), 7.46 (d, $J = 8.9$ Hz, 2H), 7.41–7.37 (m, 4H), 4.14 (s, 2H), 3.90 (s, 2H), 2.43 (s, 3H). ^{13}C NMR (125 MHz, MeOD): δ 173.57, 139.98, 136.37, 132.62, 132.17, 130.26, 129.72, 127.68, 126.52, 124.29, 122.79, 120.03, 112.65, 51.00, 43.11, 41.08. LRMS (ESI), m/z calcd for $C_{18}H_{19}N_3O$, $[M + H]^+$ 328.81, found 328.11.

4.2. Biological Assays. 4.2.1. Determination of NO Production.

BV-2 cells were seeded in 96-well plates with a density of 2×10^4 cells/well. After 24 h, cells were treated with or without LPS (1 μ g/mL) in the absence or presence of compounds at 10 μ M for 24 h. NO production in the supernatant was assessed by an NO assay kit based on the Griess reaction.³⁴ Nitrite concentrations in the cell culture medium were calculated from a prepared sodium nitrite standard curve as follows: NO inhibition (%) = $1 - (\text{sample OD} - \text{control OD}) / (\text{LPS OD} - \text{control OD}) \times 100\%$.

4.2.2. Cell Viability Assay. BV-2 cells were seeded into a 96-well plate with a density of 2×10^4 cells/well. After 24 h, cells were incubated with the compounds under investigation (10 μ M) for 24 h. Next, MTT (10 μ L, 0.5 mg/mL) was added to each well, and then the cells were maintained at 37 °C for 4 h. After this, the medium was removed, 150 μ L of DMSO was added, and the absorbance was measured at 570 nm using a microplate absorbance reader.

4.2.3. Determination of Neuroprotection against H_2O_2 . PC12 cells were seeded in a 96-well plate at 1.5×10^4 cells/well, incubated for 24 h, and subsequently treated with compounds **8c** and **8g** (5, 10, and 20 μ M) for 2 h. The cells were then treated with H_2O_2 (500 μ M) for 24 h. After this, MTT (2.5 mg/mL) was added and incubated for another 4 h at 37 °C. The medium was removed, 150 μ L of DMSO was added, and the optical density of absorbance was measured at 570 nm.

4.2.4. Measurement of TNF α with ELISA Kits. BV-2 cells were seeded in 6-well plates with a density of 2×10^4 cells/well. After 24 h, cells were treated with **8c** and **8g** with concentrations of 2 and 10 μ M, respectively, in the absence or presence of LPS (1 μ g/mL) for 24 h. Supernatant from the culture was collected to determine the concentration of TNF- α with the ELISA kits according to the protocol described in the kit instructions.

4.2.5. Western Blotting. BV-2 cells were harvested and suspended in RIPA lysis buffer containing protease and phosphatase inhibitor cocktails. The concentrations of protein were determined by a BCA protein assay kit. Equal amounts of proteins were electrophoresed in 10% SDS-PAGE and then transferred to a polyvinylidene difluoride (PVDF) Western blot membrane, which were then blocked using 5% (W/V) skim milk in TBST (Tris-buffered saline with 0.1% Tween 20) for 2 h at room temperature. The membranes were then incubated with specific primary antibodies at 4 °C overnight. After washing three times with TBST, the membranes were incubated with corresponding secondary antibodies at 4 °C for 2 h. Finally, immunoreactive signals were detected using the ChemiDoc Touch imaging system (Bio-Rad Laboratories).

4.2.6. Measurement of Neurite Outgrowth in PC-12 Cells. PC-12 cells were seeded into 24-well plates coated with PLL at a density of 1.5×10^4 cells/mL. After 24 h, the medium was replaced in differentiation medium containing 2% HS and 1% FBS for 16 h and then treated with the tested compounds and NGF in combination for 48 h. NGF (10 ng/mL) was used as a positive control. The PC12 cells were then photographed using optical microscopy. The cells bearing neurites with sizes greater than or equal to the length of the cell body were determined to be a positive cell. The cells in five random different random views were counted per well.⁹

4.2.7. Immunofluorescence. PC12 cells (1.5×10^4 cells/mL) were cultured on the climbing slices coated with PLL in 24-well plates. After replacement with medium containing 2% HS and 1% FBS for 16 h, the cells were treated with **8c** and **8g** with concentrations of 10 μ M in the presence of NGF (10 ng/mL) for 48 h. NGF (10 ng/mL) was used as a positive control. The cells were fixed with cold 4% paraformaldehyde for 20 min, permeabilized with 0.5% Triton X-100 for 30 min, and then blocked with 10% normal goat serum for 2 h at room temperature. After incubating with a primary antibody specific to β -tubulin (1:50) overnight at 4 °C, the cells were washed with TBST and incubated with the secondary antibody labeled with Alexa Fluor 488 diluted to 1:100 in TBST at 37 °C for 2 h. Following washing, the nuclei were stained by 4',6-diamidino-2-phenylindole (DAPI) and the climbing slices were washed and sealed. Images were acquired via the fluorescence microscope (OLYMPUS, Japan) with excitation/emission wavelengths of 490 nm/540 nm for the Alexa Fluor-488 and 360 nm/450 nm for the DAPI. The immunofluorescence assay of the NF- κ B p65 was as described above.

4.2.8. COX-2 Inhibition Assay. The COX-2 inhibitory activities of the compounds were measured using human COX-2 inhibitory screening assay kit (Beyotime, catalog no. S0168) according to the manufacturer's instructions. The final concentrations of the compounds were 3.125, 6.25, 12.5, 25, 50, and 100 μ M. The absorbance was measured in a microplate reader (Biotech Synergy HTX, USA) at 405 nm. IC_{50} values were calculated by the sigmoidal dose–response equation (variable slope) (GraphPad software). All of the experiments were repeated three times.

ASSOCIATED CONTENT

Supporting Information

The Supporting Information is available free of charge at <https://pubs.acs.org/doi/10.1021/acscchemneuro.1c00079>.

Predicted BBB permeability and drug-like parameters of compounds **5a–9k** and spectroscopic data of compounds **2–4**, **5a–9k** (PDF)

AUTHOR INFORMATION

Corresponding Authors

Jin-Ming Gao – Shaanxi Key Laboratory of Natural Products & Chemical Biology, College of Chemistry & Pharmacy, Northwest A&F University, Yangling 712100, P. R. China; orcid.org/0000-0003-4801-6514; Email: jinminggao@nwsuaf.edu.cn

Ding Li – Shaanxi Key Laboratory of Natural Products & Chemical Biology, College of Chemistry & Pharmacy, Northwest A&F University, Yangling 712100, P. R. China; orcid.org/0000-0003-3130-6099; Phone: +86-29-87092335; Email: jbolid@nwsuaf.edu.cn; Fax: +86-29-87092335

Authors

Wei-Wei Wang – Shaanxi Key Laboratory of Natural Products & Chemical Biology, College of Chemistry & Pharmacy, Northwest A&F University, Yangling 712100, P. R. China

Ting Liu – Shaanxi Key Laboratory of Natural Products & Chemical Biology, College of Chemistry & Pharmacy, Northwest A&F University, Yangling 712100, P. R. China

Yu-Meng Lv – Shaanxi Key Laboratory of Natural Products & Chemical Biology, College of Chemistry & Pharmacy, Northwest A&F University, Yangling 712100, P. R. China

Wu-Yang Zhang – Shaanxi Key Laboratory of Natural Products & Chemical Biology, College of Chemistry & Pharmacy, Northwest A&F University, Yangling 712100, P. R. China

Zhi-Gang Liu – Shaanxi Key Laboratory of Natural Products & Chemical Biology, College of Chemistry & Pharmacy, Northwest A&F University, Yangling 712100, P. R. China

Complete contact information is available at:

<https://pubs.acs.org/10.1021/acschemneuro.1c00079>

Author Contributions

W.-W.W. conducted the biological study and performed the experiments. T.L., Y.-M.L., and W.-Y.Z. synthesized the compounds. Z.-G.L. contributed to data analysis and interpretation. W.-W.W., J.-M.G., and D.L. conceived and designed the experiments. W.-W.W., T.L., and D.L. wrote the manuscript and revised the manuscript. All authors discussed the results and implications and commented on the manuscript at all stages.

Author Contributions

[†]W.-W.W. and T.L. contributed equally to this work.

Notes

The authors declare no competing financial interest.

ACKNOWLEDGMENTS

This work was supported by grants from the National Natural Science Foundation of China (21502152) and the Natural Science Foundation of Shaanxi Province (2019JM-334). The authors thank Life Science Research Core Services at Northwest A&F University (Luqi Li and Junmin Li) for the ESI-HRMS data.

REFERENCES

- (1) Siew, J. J., Chen, H. M., Chen, H. Y., Chen, H. L., Chen, C. M., Soong, B. W., Wu, Y. R., Chang, C. P., Chan, Y. C., Lin, C. H., et al. (2019) Galectin-3 is required for the microglia-mediated brain inflammation in a model of Huntington's disease. *Nat. Commun.* 10 (1), 3473.
- (2) Gilhus, N. E., and Deuschl, G. (2019) Neuroinflammation — a common thread in neurological disorders. *Nat. Rev. Neurol.* 15 (8), 429–430.
- (3) Ransohoff, R. M., and Perry, V. H. (2009) Microglial physiology: Unique stimuli, specialized responses. *Annu. Rev. Immunol.* 27 (1), 119–145.
- (4) Kaur, N., Chugh, H., Sakharkar, M. K., Dhawan, U., Chidambaram, S. B., and Chandra, R. (2020) Neuroinflammation mechanisms and phytotherapeutic intervention: A systematic review. *ACS Chem. Neurosci.* 11 (22), 3707–3731.
- (5) Afridi, R., Kim, J. H., Rahman, M. H., and Suk, K. (2020) Metabolic regulation of glial phenotypes: Implications in neuron-glia interactions and neurological disorders. *Front. Cell. Neurosci.* 14, 20.
- (6) Gupta, N., Shyamasundar, S., Patnala, R., Karthikeyan, A., Arumugam, T. V., Ling, E. A., and Dheen, S. T. (2018) Recent progress in therapeutic strategies for microglia-mediated neuroinflammation in neuropathologies. *Expert Opin. Ther. Targets* 22 (9), 765–781.
- (7) Yang, T., Velagapudi, R., and Terrando, N. (2020) Neuroinflammation after surgery: From mechanisms to therapeutic targets. *Nat. Immunol.* 21 (11), 1319–1326.
- (8) McAllister, A. K. (2001) Neurotrophins and neuronal differentiation in the central nervous system. *Cell. Mol. Life Sci.* 58 (8), 1054–1060.
- (9) Zhao, J., Cheng, Y. Y., Fan, W., Yang, C. B., Ye, S. F., Cui, W., Wei, W., Lao, L. X., Cai, J., Han, Y. F., et al. (2015) Botanical drug puerarin coordinates with nerve growth factor in the regulation of neuronal survival and neurite extension via activating ERK1/2 and PI3K/Akt signaling pathways in the neurite extension process. *CNS Neurosci. Ther.* 21 (1), 61–70.
- (10) Dawbarn, D., and Allen, S. J. (2003) Neurotrophins and neurodegeneration. *Neuropathol. Appl. Neurobiol.* 29 (3), 211–230.
- (11) Liao, K. K., Wu, M. J., Chen, P. Y., Huang, S. W., Chiu, S. J., Ho, C. T., and Yen, J. H. (2012) Curcuminoids promote neurite outgrowth in PC12 cells through MAPK/ERK- and PKC-dependent pathways. *J. Agric. Food Chem.* 60 (1), 433–443.
- (12) Spedding, M., and Gressens, P. (2008) Neurotrophins and cytokines in neuronal plasticity. *Novartis Found Symp.* 289, 222–237.
- (13) Price, R. D., Milne, S. A., Sharkey, J., and Matsuoka, N. (2007) Advances in small molecules promoting neurotrophic function. *Pharmacol. Ther.* 115 (2), 292–306.
- (14) Savelieff, M. G., Nam, G., Kang, J., Lee, H. J., Lee, M., and Lim, M. H. (2019) Development of multifunctional molecules as potential therapeutic candidates for Alzheimer's disease, Parkinson's disease, and amyotrophic lateral sclerosis in the last decade. *Chem. Rev.* 119 (2), 1221–1322.
- (15) Tang, G., Liu, X., Ma, N., Huang, X., Wu, Z. L., Zhang, W., Wang, Y., Zhao, B. X., Wang, Z. Y., Ip, F. C. F., et al. (2016) Design and synthesis of dimeric securinine analogues with neurotogenic activities. *ACS Chem. Neurosci.* 7 (10), 1442–1451.
- (16) De Simone, A., La Pietra, V., Betari, N., Petragani, N., Conte, M., Daniele, S., Pietrobono, D., Martini, C., Petralla, S., Casadei, R., et al. (2019) Discovery of the first-in-class GSK-3 β /HDAC dual inhibitor as disease-modifying agent to combat Alzheimer's disease. *ACS Med. Chem. Lett.* 10 (4), 469–474.
- (17) Xu, Y., Wei, H., Wang, J., Wang, W., and Gao, J. (2019) Synthesis of andrographolide analogues and their neuroprotection and neurite outgrowth-promoting activities. *Bioorg. Med. Chem.* 27 (11), 2209–2219.
- (18) Sravanthi, T. V., and Manju, S. L. (2016) Indoles — a promising scaffold for drug development. *Eur. J. Pharm. Sci.* 91, 1–10.
- (19) Chadha, N., and Silakari, O. (2017) Indoles as therapeutics of interest in medicinal chemistry: Bird's eye view. *Eur. J. Med. Chem.* 134, 159–184.
- (20) Hixson, S. S., Franke, L. A., Gere, J. A., and Xing, Y. D. (1988) Arylcyclopropane photochemistry. Unusual aromatic substituent effects on the photochemical rearrangement of (2-arylcyclopropyl)-

methyl acetates to 1-arylhomoolyl acetates. *J. Am. Chem. Soc.* 110 (11), 3601–3610.

(21) Chen, K., Zhang, Y. L., Fan, J., Ma, X., Qin, Y. J., and Zhu, H. L. (2018) Novel nicotinoyl pyrazoline derivatives bearing N-methyl indole moiety as antitumor agents: Design, synthesis and evaluation. *Eur. J. Med. Chem.* 156, 722–737.

(22) Mahboobi, S., Grothus, G., and Meindl, W. (1994) Antimykobakteriell wirksame indolderivate. *Arch. Pharm. (Weinheim, Ger.)* 327 (2), 105–114.

(23) Fan, X., Li, J., Deng, X., Lu, Y., Feng, Y., Ma, S., Wen, H., Zhao, Q., Tan, W., Shi, T., et al. (2020) Design, synthesis and bioactivity study of N-salicyloyl tryptamine derivatives as multifunctional agents for the treatment of neuroinflammation. *Eur. J. Med. Chem.* 193, 112217.

(24) Cao, C. Y., Zhang, C. C., Shi, X. W., Li, D., Cao, W., Yin, X., and Gao, J. M. (2018) Sarcodonin G derivatives exhibit distinctive effects on neurite outgrowth by modulating NGF signaling in PC12 cells. *ACS Chem. Neurosci.* 9 (7), 1607–1615.

(25) Tan, S., Wood, M., and Maher, P. (1998) Oxidative stress induces a form of programmed cell death with characteristics of both apoptosis and necrosis in neuronal cells. *J. Neurochem.* 71 (1), 95–105.

(26) Wang, F., Liu, Q., Wang, W., Li, X., and Zhang, J. (2016) A polysaccharide isolated from *Cynomorium songaricum* Rupr. protects PC12 cells against H₂O₂-induced injury. *Int. J. Biol. Macromol.* 87, 222–228.

(27) Xia, W., Luo, P., Hua, P., Ding, P., Li, C., Xu, J., Zhou, H., and Gu, Q. (2019) Discovery of a new pterocarpan-type antineuroinflammatory compound from *Sophora tonkinensis* through suppression of the TLR4/NFκB/MAPK signaling pathway with PU.1 as a potential target. *ACS Chem. Neurosci.* 10 (1), 295–303.

(28) Qi, G., Mi, Y., Fan, R., Li, R., Liu, Z., and Liu, X. (2019) Nobiletin protects against systemic inflammation-stimulated memory impairment via MAPK and NF-κB signaling pathways. *J. Agric. Food Chem.* 67 (18), 5122–5134.

(29) Mroueh, M., Faour, W. H., Shebawy, W. N., Daher, C. F., Ibrahim, T. M., and Ragab, H. M. (2020) Synthesis, biological evaluation and modeling of hybrids from tetrahydro-1*H*-pyrazolo[3,4-*b*]quinolines as dual cholinesterase and COX-2 inhibitors. *Bioorg. Chem.* 100, 103895.

(30) Pardridge, W. M. (2005) The blood-brain barrier: Bottleneck in brain drug development. *NeuroRx* 2 (1), 3–14.

(31) Cheng, F., Li, W., Zhou, Y., Shen, J., Wu, Z., Liu, G., Lee, P. W., and Tang, Y. (2012) admetSAR: A comprehensive source and free tool for assessment of chemical ADMET properties. *J. Chem. Inf. Model.* 52 (11), 3099–3105.

(32) Hanke, T., Rörsch, F., Thieme, T. M., Ferreiros, N., Schneider, G., Geisslinger, G., Proschak, E., Grösch, S., and Schubert-Zsilavecz, M. (2013) Synthesis and pharmacological characterization of benzenesulfonamides as dual species inhibitors of human and murine mPGES-1. *Bioorg. Med. Chem.* 21 (24), 7874–7883.

(33) Zhan, W., Ji, L., Ge, Z. M., Wang, X., and Li, R. T. (2018) A continuous-flow synthesis of primary amides from hydrolysis of nitriles using hydrogen peroxide as oxidant. *Tetrahedron* 74 (13), 1527–1532.

(34) Yin, H., Dan, W. J., Fan, B. Y., Guo, C., Wu, K., Li, D., Xian, K. F., Pescitelli, G., and Gao, J. M. (2019) Anti-inflammatory and α-Glucosidase inhibitory activities of labdane and norlabdane diterpenoids from the rhizomes of *amomum villosum*. *J. Nat. Prod.* 82 (11), 2963–2971.